Design, Synthesis and Biological Evaluation of 6-Substituted Thieno[3,2-*d*]pyrimidine Analogues as Dual Epidermal Growth Factor Receptor Kinase and Microtubule Inhibitors

Romeo Romagnoli*†, Filippo Prencipe†, Paola Oliva†, Stefania Baraldi†, Pier Giovanni Baraldi†, Santiago Schiaffino Ortega[ψ], Mariem Chayah[ψ], Maria Kimatrai Salvador[ψ], Luisa Carlota Lopez-Cara*[ψ], Andrea Brancale[§], Salvatore Ferla[§], Ernest Hamel[‡], Roberto Ronca[§§], Roberta Bortolozzi††, Elena Mariotto††, Elena Mattiuzzo†† and Giampietro Viola*††,[ψψ]

[†]*Dipartimento di Scienze Chimiche e Farmaceutiche, Università degli Studi di Ferrara, Via Luigi Borsari 46, 44121 Ferrara, Italy;*

[ψ]*Departamento de Química Farmacéutica y Orgánica, Facultad de Farmacia, Campus de Cartuja s/n, 18071, Granada, Spain;*

[§]*School of Pharmacy and Pharmaceutical Sciences, Cardiff University, King Edward VII Avenue, Cardiff, CF10 3NB, UK;*

[‡]*Screening Technologies Branch, Developmental Therapeutics Program, Division of Cancer Treatment and Diagnosis, Frederick National Laboratory for Cancer Research, National Cancer Institute, National Institutes of Health, Frederick, Maryland 21702, USA;*

[§§]*Dipartimento di Medicina Molecolare e Traslazionale Unità di Oncologia Sperimentale ed Immunologia, Università di Brescia, 25123 Brescia, Italy;* ††*Dipartimento di Salute della Donna e del Bambino, Laboratorio di Oncoematologia, Università di Padova, 35131 Padova, Italy*

[ψψ] *Istituto di Ricerca Pediatrica (IRP), Corso Stati Uniti 4, 35128 Padova, Italy*

Abstract: The clinical evidence for the success of tyrosine kinase inhibitors in combination with microtubule targeting agents prompted us to design and to develop single agents which possess both epidermal growth factor receptor (EGFR) kinase and tubulin polymerization inhibitory properties. A series of 6-aryl/heteroaryl-4-(3',4',5'-trimethoxyanilino)thieno[3,2-*d*]pyrimidine derivatives were discovered as novel dual tubulin polymerization and EGFR kinase inhibitors. The 4-(3',4',5'-trimethoxyanilino)-6-(*p*-tolyl)thieno[3,2-*d*]pyrimidine derivative **6g** was the most potent compound of the series as an antiproliferative agent, with IC_{50} values in the single- or double-digit nanomolar range. This derivative bound to the colchicine site of tubulin and inhibited tubulin polymerization at submicromolar concentrations and inhibited EGFR activity with an IC_{50} of 30 nM. Our data suggested that the excellent *in vitro* and *in vivo* profile of **6g** may be derived from its dual inhibition of tubulin polymerization and EGFR kinase.

INTRODUCTION

The microtubule system of eukaryotic cells involves the non-covalent polymerization of α- and β-tubulin heterodimers and acts as an essential element of the cytoskeleton. Microtubules are crucial for a variety of fundamental cellular processes, including the formation of the mitotic spindle during mitosis, formation and maintenance of cell shape, organization of intracellular architecture, secretion, cellular transport, regulation of motility and organelle transport inside the cell.[1] Given their significant role in these cellular functions, microtubules are an attractive molecular target for anticancer drug discovery and are still among the most reliable chemotherapeutics.[2] Numerous chemically diverse antimitotic agents, many of which are natural products, interact specifically with tubulin and alter tubulin polymerization.[3] Moreover, several small molecules inhibiting tubulin polymerization are able to damage the already existing vasculature in developing tumors, acting as vascular disrupting agents (VDAs).[4]

Combretastatin A-4 (CA-4, **1a**, Figure 1), isolated from the bark of the South African tree *Combretum caffrum,*[5] is one of the well-known natural tubulin binding molecules affecting microtubule dynamics. CA-4 strongly inhibits the polymerization of tubulin by binding to the colchicine site.[6] The disodium phosphate prodrug of CA-4 (CA-4P, **1b**) is water-soluble, and there have been promising results with **1b** as a tumor VDA in phase II clinical trials.[7] Its structural simplicity, along with its ability to selectively damage tumor neovasculature, makes CA-4 of great interest from the medicinal chemistry point of view.[8]

A growing body of evidence showing that antimitotic agents, and in particular microtubule destabilizing drugs, have multiple effects beyond mitosis.[9] Several lines of evidence suggested mixed mechanisms that are not so far fully understood to explain the activities of tubulin binding agents, and these mechanisms probably extend beyond simple antimitotic effects. Moreover, there is evidence that the efficacy of microtubule targeting agents also involve interphase effects.[10]

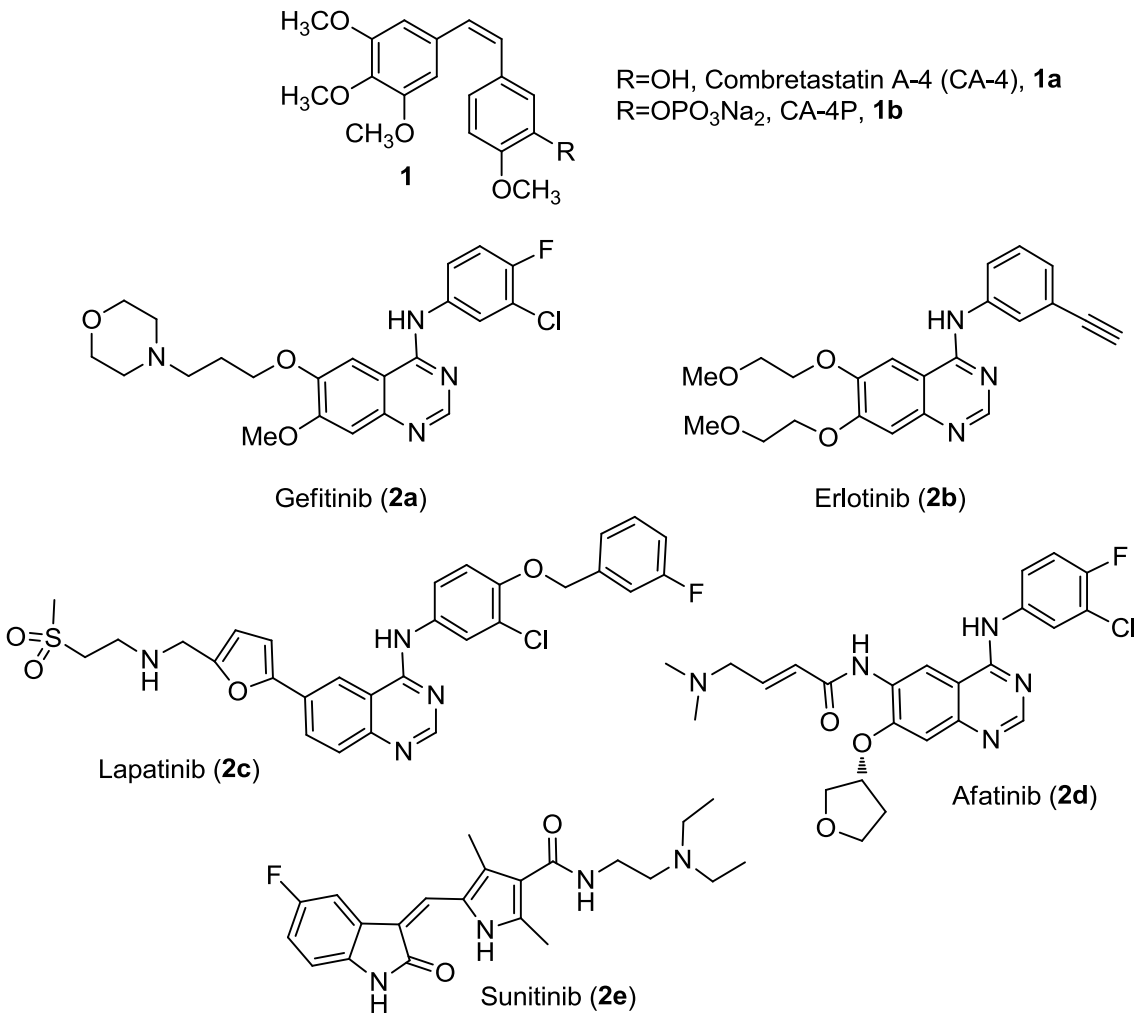

Figure 1. Structures of tubulin depolymerizing agents CA-4 and CA-4P and selected EGFR (**2a-d**) and VEGFR-2 (**2e**) tyrosine kinase inhibitors.

The epidermal growth factor receptor (EGFR) is a *trans*-membrane bound tyrosine kinase involved in cellular signal-transduction pathways, and it plays a crucial role in the regulation of essential functions that affect tumor growth and progression. These include cell proliferation, differentiation, migration, apoptosis and angiogenesis.[11] The EGFR is a component of the ErbB family, which consists of four receptors: the EGFR (ErbB1, HER1), the human epidermal growth factor receptor-2 (HER2, ErbB-2), the human epidermal growth factor receptor-3 (HER3, ErbB3) and the human epidermal growth factor receptor-4 (HER4, ErbB4).[12] Among the known receptor tyrosine kinases (RTKs), the ErbB family, in particular EGFR and HER2 have been extensively studied and clinically validated as targets for cancer therapies, being over-expressed in a wide number of human tumors

and associated with cancer proliferation, angiogenesis and metastasis.[13] In the absence of ligand, EGFR exists as monomers on the cell surface, while binding of ligand to EGFR leads to the formation of receptor homo- and heterodimers, depending on whether EGFR is dimerized with another EGFR or with other ErbB family members, respectively.[14] There are currently eight drugs approved by the FDA targeting this family: four monoclonal antibodies (trastuzumab, cetuximab, panitumumab and pertuzumab) and four small-molecule inhibitors based on a central 4-aminoarylquinazoline core [Gefitinb (**2a**), erlotinib (**2b**), lapatinib (**2c**) and afatinib (**2d**)].[15] These latter synthetic EGFR inhibitors have been approved by the FDA for the treatment of patients with non-small cell lung cancer (NSCLC).[16] Unfortunately, the duration of benefit derived from tyrosine kinase inhibitor based-therapy is relatively short, due to the development of acquired resistance.[17a] The development of multi-targeted inhibitors represents a valid approach to overcome the acquired drug resistance to tyrosine kinase inhibitors.[17b] Twelve clinical trials were found on clinicaltrials.gov site (accessed in October 2018) in which the FDA approved the EGFR kinase inhibitors gefitinib, erlotinib and lapatinib being used in combination with the microtubule targeting agents docetaxel, vinorelbine, paclitaxel and other chemotherapeutic agents for the treatment of a variety of cancers including, lung cancer, head and neck cancer and hepatocellular carcinoma.[18]

A large number of thienopyrimidine derivatives have been reported to show remarkable antitumor activity against different cancer types by means of inhibiting multiple enzymes, as well as by modulating the activity of many receptors.[19] In an effort to develop non-quinazoline EGFR inhibitors, using the strategy known as "scaffold hopping", bioisosteric thieno[2,3-*d*]pyrimidine and thieno[3,2-*d*]pyrimidine scaffolds have been reported as interesting structural elements employed for the development of novel EGFR or EGFR and vascular growth factor receptor-2 (VEGFR-2) dual inhibitors.[20]

Munchhof et al. reported the design and structure-activity relationship (SAR) of a series of 6-aryl substituted thieno[3,2-*d*]pyrimidines with general structure **3**, identified as VEGFR-2 and EGFR dual inhibitors (Figure 2).[21] Kemnitzer and colleague reported the discovery of *N*-methyl-4-

(methoxyanilino)thieno[3,2-*d*]pyrimidine **4** as a potent apoptosis inducer through inhibition of tubulin assembly, with IC_{50}<1 μM in the tubulin polymerization assay.[22] This compound inhibited the growth of a panel of five cancer cell lines (T-47D, HT-29, H-1299, MX-1 and MDAAMB 435) with IC_{50} values ranging from 4 to 40 nM. Much research has been conducted on the structural modification of the thieno[3,2-*d*]pyrimidine skeleton, with the 4-, 6- and 7-positions as the main targets for chemical modifications to increase antitumor activity.[23]

Lin et al. have also reported a series of 2,7-diaminothiazolo[4,5-*d*]pyrimidines with general formula **5**, with various structural modifications at the 2- and 7-positions, as potent EGFR inhibitors, with IC_{50} values ranging from micromolar to single digit nanomolar.[24] Compound **5a**, characterized by potent and selective EGFR activity (IC_{50}: 12 nM), proved to be active *in vitro* as an antiproliferative agent against the human ovarian adenocarcinoma (SK-OV-3) cell line, with an IC_{50} of 0.57 μM. Unfortunately, compound **5a** showed no *in vivo* antitumor efficacy in a tumor xenograft model in nude mice.

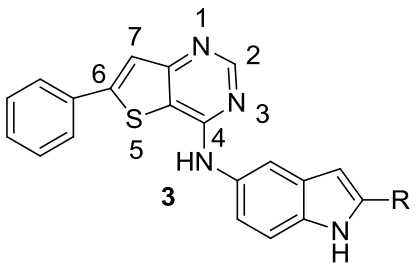

3

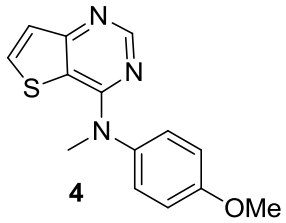

4

3a, R=H, VEGFR-2 IC_{50}: 80 nM, EGFR IC_{50}: 3 nM
3b, R=Me, VEGFR-2 IC_{50}: 140 nM, EGFR IC_{50}: 100 nM

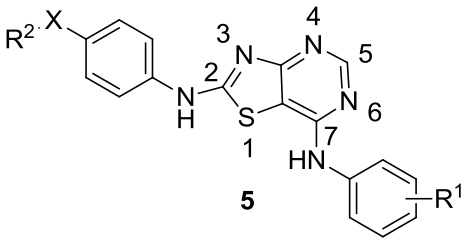

5

X=nothing, O, CH_2 or CH_2CH_2
R^1=halogen
R^2=H, SO_2NH_2, morpholine, pyrrolidine, piperidine, imidazole.
5a, X=CH_2, R^1=3'-Cl, 4'-F; R^2=*N*-morpholine

Figure 2. Chemical structures of representative thieno[3,2-*d*]pyrimidines and thiazolo[4,5-*d*]pyrimidines as known tubulin polymerization (**4**) and EGFR kinase (**3** and **5**) inhibitors.

These results led us to start a pharmacophore exploration and optimization effort around the thieno[3,2-*d*]pyrimidine skeleton, which was maintained as the key scaffold for the discovery of new antitumor agents. We replaced the 5'-aminoindole side chain at the C-4 position of 6-phenylthieno[2,3-*d*]pyrimidine derivatives with general structure **3** with a 3',4',5'-trimethoxyanilino moiety, to furnish a first series of 4-(3',4',5'-trimethoxyanilino)-6-aryl/heteroaryl thieno[3,2-*d*]pyrimidine derivatives with general structure **6** (Figure 3). By maintaining the 3',4',5'-trimethoxyanilino group at the 4-position, the first stage of our study was to evaluate the steric and electronic effects of different substituents on the benzene portion at the C-6 position of the 4-(3',4',5'-trimethoxyanilino)thieno[2,3-*d*]pyrimidine nucleus. Besides the hydrogen, the examined substituents included electron withdrawing groups (EWGs), such as F, Cl, Br, I and NO_2, and the electron releasing methyl and methoxy groups (ERGs). The bioisosteric replacement of phenyl with the thien-2-yl ring was also explored.

Because it is well known that the trimethoxyphenyl skeleton is the characteristic structural requirement to maximize the activity of a large series of inhibitors of tubulin polymerization inhibitors, such as colchicine, CA-4 and podophyllotoxin,[25] all newly prepared compounds retain the 3',4',5'-trimethoxyanilino moiety at the common C-4 position of the thieno[2,3-*d*]pyrimidine and isomeric thieno[3,2-*d*]pyrimidine nucleus, as well as at the C-7 position of the thiazolo[4,5-*d*]pyrimidine system.

In the second small series of compounds, the thiophene nucleus was replaced by the bioisosteric thiazole ring, to obtain the derivatives **7a-d**, characterized by the presence of an anilino moiety at its C-7 position. The electron-withdrawing chlorine atom (**7b**) and the electron-releasing methyl and methoxy groups (**7c** and **7d**, respectively) were introduced at the *para*-position of the phenyl portion of the anilino moiety.

In a third series of compounds **8a-l**, we explored the replacement of the thieno[3,2-*d*]pyrimidine system, which characterizes derivatives with general structure **6**, by the isomeric thieno[2,3-*d*]pyrimidine nucleus. The SAR was investigated by the insertion of different substituents (Cl, Me or

OMe) on the phenyl at the C-5 or C-6 positions of the 4-(3',4',5'-trimethoxyanilino)thieno[2,3-*d*]pyrimidine core.

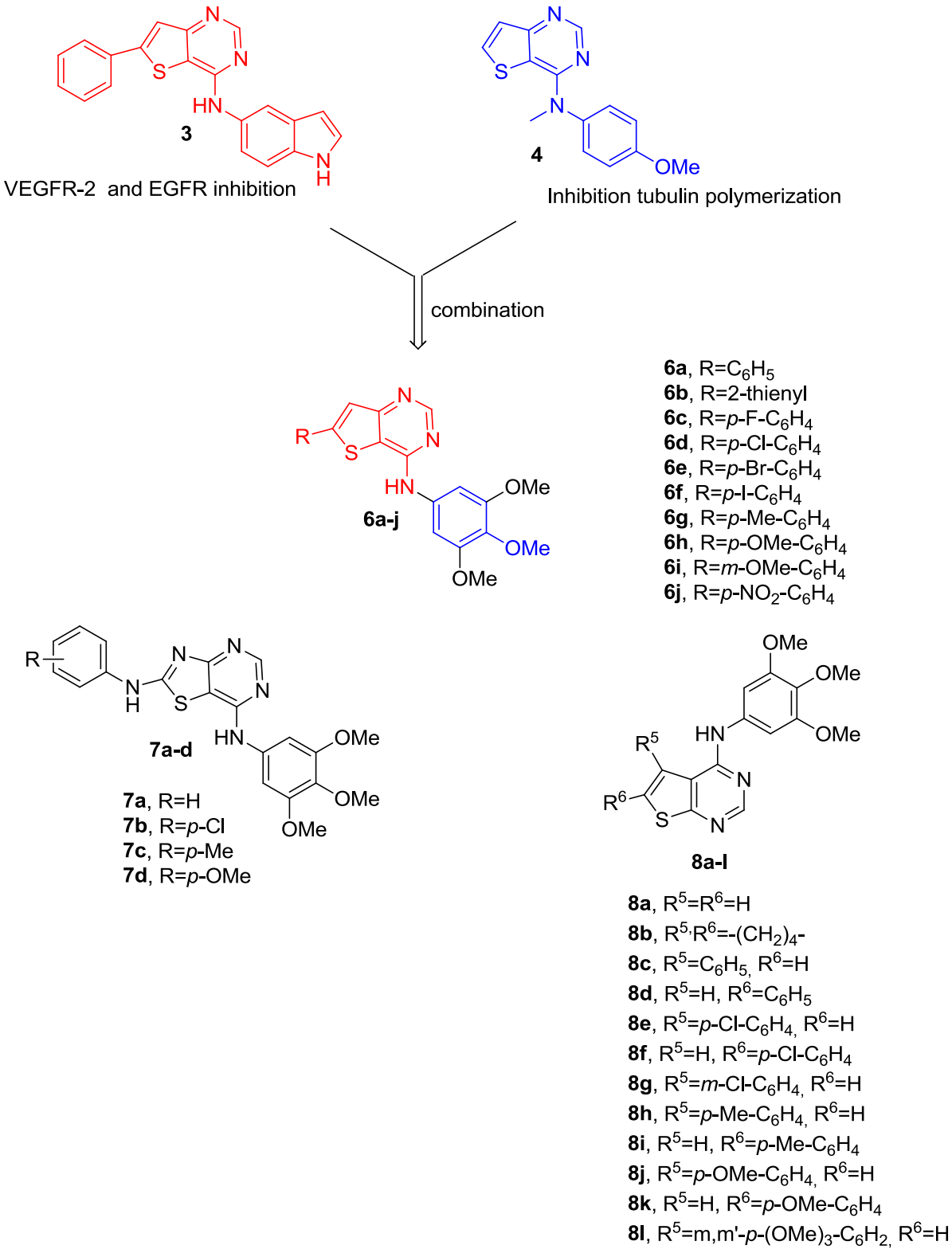

Figure 3. Design strategy for thieno[3,2-*d*]pyrimidines **6a-j**. Target compounds containing the thiazolo[4,5-*d*]pyrimidine (**7a-d**) and thieno[2,3-*d*]pyrimidine (**8a-l**) scaffolds.

These three series of compounds, obtained by replacing the thieno[3,2-*d*]pyrimidine scaffold with the isomeric thieno[2,3-*d*]pyrimidine and the bioisosteric thiazolo[4,5-*d*]pyrimidine skeletons, were designed to determine the potential of incorporating in a single molecule both VEGFR-2 and/or EGFR kinase inhibition and antitubulin activity.

The biososteric replacement of the thiophene ring of the structure motif of the thieno[2,3-*d*]pyrimidine nucleus with a furan or pyrrole provided two series of furo[2,3-*d*]pyrimidine and pyrrolo[3,2-*d*]pyrimidine derivatives, respectively, identified by Gangjee et al. as multitarget receptor tyrosine kinase and microtubule inhibitors.[26-28] A literature search also revealed that recent studies have yielded different series of chemically diverse small molecules acting as EGFR kinase and tubulin polymerization inhibitors derived from anthranilic acid[29] or benzo[*b*]furan[30] or obtained by replacing the quinazoline core of compounds **2a-d** with a quinazolinone[31,32] or triazolo[4,3-*a*]quinoxaline[33] scaffold.

RESULTS AND DISCUSSION

Chemistry. Preparation of thieno[3,2-*d*] pyrimidine and thiazolo[4,5-*d*]pyrimidine derivatives **6a-j** and **7a-d**, respectively, was accomplished using the general convergent synthetic route shown in Scheme 1. Cyclization of methyl 5-aryl/heteroayl-3-aminothiophene-2-carboxylate and ethyl 2-anilino-4-aminothiazole-5-carboxylate **9a-j** and **9k-n**, respectively, with formamide ($HCONH_2$) yielded the corresponding 6-aryl/heteroaryl-thieno[3,2-*d*]pyrimidin-4(3*H*)-ones **10a-j** and 2-arylaminothiazolo[4,5-*d*]pyrimidin-7(6*H*)-ones **10k-n**. The subsequent chlorination of the carbonyl group with phosphorus oxychloride ($POCl_3$) provided 4-chlorothieno[3,2-*d*]pyrimidine and 7-chlorothiazolo[4,5-*d*]pyrimidine derivatives **11a-j** and **11k-n**, respectively. Finally, the nucleophilic substitution with 3,4,5-trimethoxyaniline in refluxing isopropanol furnished the final compounds **6a-j** and **7a-d**, respectively.

Scheme 1. Synthesis of thieno[3,2-*d*]pyrimidines **6a-j** and thiazolo[4,5-*d*]pyrimidines **7a-d**[a]

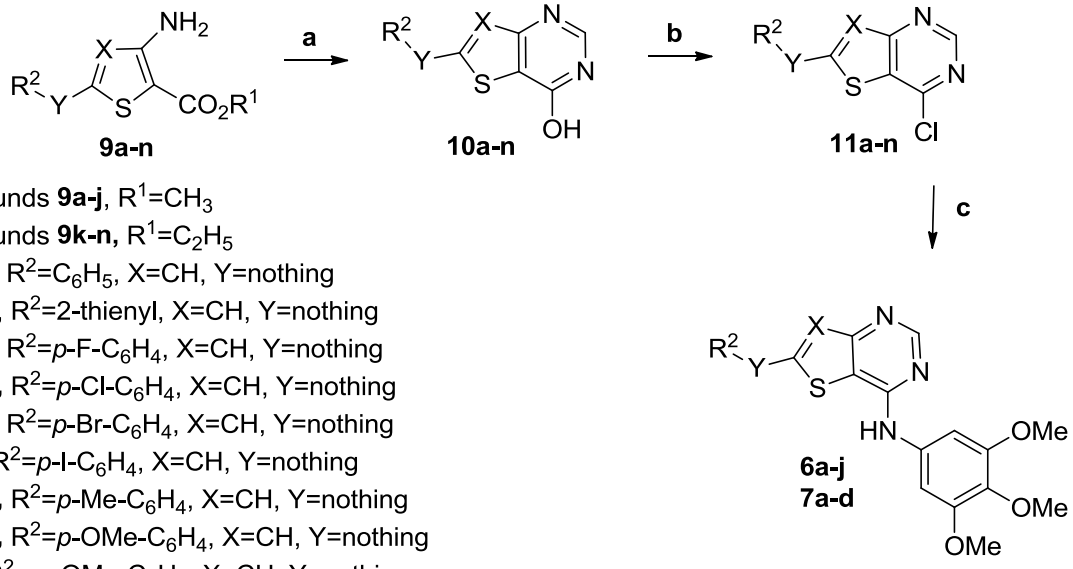

9a-n **10a-n** **11a-n** **6a-j** **7a-d**

For compounds **9a-j**, R^1=CH_3
For compounds **9k-n,** R^1=C_2H_5
6a, **9a-11a**, R^2=C_6H_5, X=CH, Y=nothing
6b, 9b-11b, R^2=2-thienyl, X=CH, Y=nothing
6c, 9c-11c, R^2=*p*-F-C_6H_4, X=CH, Y=nothing
6d, 9d-11d, R^2=*p*-Cl-C_6H_4, X=CH, Y=nothing
6e, 9e-11e, R^2=*p*-Br-C_6H_4, X=CH, Y=nothing
6f, 9f-11f, R^2=*p*-I-C_6H_4, X=CH, Y=nothing
6g, 9g-11g, R^2=*p*-Me-C_6H_4, X=CH, Y=nothing
6h, 9h-11h, R^2=*p*-OMe-C_6H_4, X=CH, Y=nothing
6i, 9i-11i, R^2=*m*-OMe-C_6H_4, X=CH, Y=nothing
6j, 9j-11j, R^2=*p*-NO_2-C_6H_4, X=CH, Y=nothing
7a, 9k-11k, R^2=C_6H_5, X=N, Y=NH
7b, **9l-11l**, R^2=*p*-Cl-C_6H_4, X=N, Y=NH
7c, **9m-11m**, R^2=*p*-Me-C_6H_4, X=N, Y=NH
7d, **9n-11n,** R^2=*p*-OMe-C_6H_4, X=N, Y=NH

[a]*Reagents and conditions*. **a**: $HCONH_2$, 180 °C; **b**: $POCl_3$, 110 °C; **c**: 3,4,5-trimethoxyaniline, isopropanol, reflux.

The isomeric 4-(3',4',5'-trimethoxyanilino)-thieno[2,3-*d*]pyrimidine derivatives **8a-l** were synthesized following the procedure reported in Scheme 2. Thieno[2,3-*d*]pyrimidin-4(3*H*)-one derivatives **13a-l** variously substituted at their C-5 or C-6 position were prepared by the cyclocondensation of ethyl 2-aminothiophene-3-carboxylate derivatives **12a-l** with $HCONH_2$ at 180 °C for 8-12 h. These intermediates were subjected to chlorination by the action of $POCl_3$ at reflux to furnish the 4-chlorothieno[2,3-*d*]pyrimidine analogues **14a-l**. The final step of the synthesis involved nucleophilic displacement of the 4-chloride atom of **14a-l** with 3,4,5-trimethoxyaniline in refluxing isopropanol to obtain the 4-(3',4',5'-trimethoxyanilino)thieno[3,2-*d*]pyrimidine derivatives **8a-l**.

Scheme 2. Synthesis of thieno[2,3-*d*]pyrimidines (**8a-l**)[a]

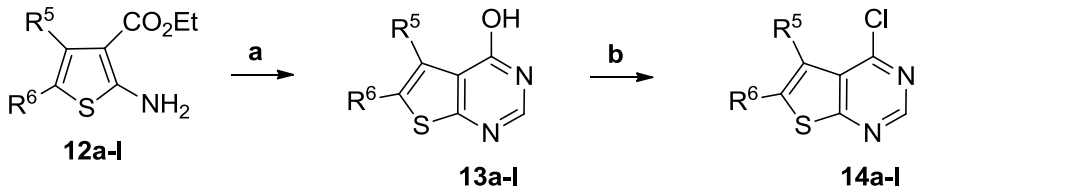

8a, **12a-14a**, R^5=R^6=H
8b, **12b-14b**, R^5,R^6=-$(CH_2)_4$-
8c, **12c-14c**, R^5=C_6H_5, R^6=H
8d, **12d-14d**, R_5=H, R^6=C_6H_5
8e, **12e-14e**, R^5=*p*-Cl-C_6H_4, R^6=H
8f, **12f-14f**, R^5=H, R^6=*p*-Cl-C_6H_4
8g, **12g-14g**, R^5=*m*-Cl-C_6H_4, R^6=H
8h, **12h-14h**, R^5=*p*-Me-C_6H_4, R^6=H
8i, **12i-14i**, R^5=H, R^6=*p*-Me-C_6H_4
8j, **12j-14j**, R^5=*p*-OMe-C_6H_4, R^6=H
8k, **12k-14k**, R^5=H, R^6=*p*-OMe-C_6H_4
8l, **12l-14l**, R^5=m,m'-*p*-$(OMe)_3$-C_6H_2, R^6=H

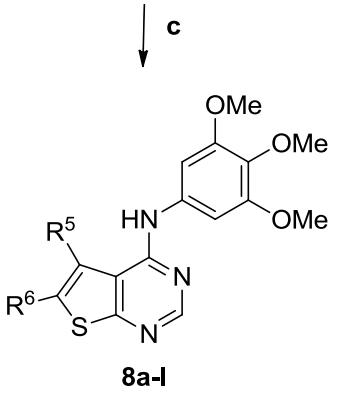

[a]*Reagents and conditions*. **a**: $HCONH_2$, 180 °C; **b**: $POCl_3$, 110 °C; **c**: 3,4,5-trimethoxyaniline, isopropanol, reflux.

In vitro **antiproliferative activities.** Table 1 summarizes the antiproliferative effects of 4-(3',4',5'-trimethoxyanilino)-6-substituted thieno[3,2-*d*]pyrimidine derivatives **6a-j** against a panel of five human cancer cell lines [including EGFR wild-type ($EGFR^{wt}$) NSCLC A549 cells], using CA-4 as the reference compound. The corresponding thieno[2,3-*d*]pyrimidine isomers **7a-d** and the 2-anilino-7-(3',4',5'-trimethoxyanilino)thiazolo[4,5-*d*]pyrimidine **8a-l** were also evaluated for their activities on the same panel of cells, but because they were all inactive (IC_{50}>10 μM), with only a few exceptions on selected cancer cell lines (derivatives **6h**, **6k** and **6l**), these biological data are presented in the Supplementary Information section as Table 1s and Table 2s, respectively.

Table 1. In vitro cell growth inhibitory effects of compounds **6a-j** and CA-4

Compound	IC_{50} [a](μM)				
	A549	HeLa	HT29	Jurkat	RS4;11
6a	2.3±0.7	0.17±0.02	0.35±0.06	0.01±0.006	0.26±0.10
6b	5.1±1.9	1.7±0.8	0.21±0.07	0.08±0.03	0.36±0.1
6c	13.5±3.0	0.45±0.09	1.9±0.8	0.26±0.04	1.9±0.3
6d	0.60±0.11	0.09±0.03	0.087±0.033	0.003±0.001	0.005±0.002
6e	0.53±0.16	0.22±0.09	0.15±0.04	0.03±0.005	0.19±0.04
6f	0.77±0.26	0.28±0.15	0.25±0.13	0.30±0.06	0.17±0.04
6g	0.019±0.008	0.001±0.0005	0.02±0.007	0.001±0.0005	0.002±0.001
6h	0.43±0.13	0.17±0.08	0.06±0.04	0.005±0.001	0.004±0.001
6i	8.8±1.9	3.2±0.1	3.3±0.8	3.0±1.0	5.4±1.3
6j	1.1±0.3	4.9±1.4	6.3±1.4	2.0±0.3	1.3±0.4
CA-4	0.18±0.05	0.004±0.0001	3.1±0.1	0.005±0.0001	0.001±0.0001

[a]IC_{50}= compound concentration required to inhibit tumor cell proliferation by 50%. Data are expressed as the mean ± SE from the dose-response curves of at least three independent experiments.

The unsubstituted phenyl derivative **6a** was weakly active (IC_{50}: 2.3 μM) against A549, moderately potent against HeLa, HT-29 and RS4;11 with IC_{50} values of 0.17, 0.35 and 0.26 μM, respectively, but showed high activity (IC_{50}: 10 nM) against Jurkat cells. The bioisosteric 2-thienyl analogue **6b** was 2-, 8- and 10- fold less active than **6a** against A549, Jurkat and HeLa cells, respectively, while the difference in potency between **6a** and **6b** was minimal in RS4;11 cells. Only in HT29 cells **6a** was less active than **6b**, with IC_{50} values of 0.35 and 0.21 μM, respectively.

The introduction of electron-releasing or electron-withdrawing substituents at the *para*-position of the phenyl ring at the C-6 position of the thieno[3,2-*d*]pyrimidine nucleus appeared to have considerable biological effects, enhancing antiproliferative activity compared with the unsubstituted phenyl analogue **6a**. These compounds include the *p*-Cl (**6d**; IC_{50}: 3-600 nM), *p*-Me (**6g**; IC_{50}: 1-20 nM) and *p*-OMe (**6h**; IC_{50}: 4-430 nM) derivatives. The *p*-tolyl derivative **6g** displayed the strongest growth inhibitory activity against A549, HeLa, HT29, Jurkat and RS4:11, with IC_{50} values of 19, 1, 20, 1 and 2 nM, respectively.

The introduction of a fluorine atom at the *para*-position of the phenyl ring (compound **6c**) caused a reduction of activity of 2-26-fold relative to the unsubstituted phenyl derivative **6a**, while the presence of other halogen groups led to an improvement in antiproliferative activity. Increasing the size of halide from fluorine to chlorine, resulting in compound **6d**, produced a 5- to 87-fold increase in antiproliferative activity in the five cell lines. Replacing chlorine with bromine (**6e**), reduced activity 2-38-fold against four of the five cancer cell lines, but **6d** and **6e** were equally potent against A549 cells. For the *p*-Br and *p*-I derivatives **6e** and **6f**, respectively, nearly identical activities were observed in three of the five cancer cell lines, the exception being the HT-29 and Jurkat cells, in which **6f** was 2- and 10-fold more potent than **6e**, respectively.

The small and weak electron-releasing methyl group at the *para*-position of the phenyl ring, to yield derivative **6g**, improved significantly antiproliferative activity relative to **6a**. Derivative **6g** exhibited the greatest cell growth inhibitory effects among the tested compounds, with IC_{50} values of 1-20 nM against all cell lines, as compared with the range 0.8-3100 nM obtained with CA-4. Compound **6g** was equipotent with CA-4 against RS4;11 cells, while it was from 2- to $1.5x10^5$ times more active against the other four cancer cell lines.

Replacement of the methyl group of **6g** with a more electron-releasing methoxy group at the *para*-position of the phenyl ring (compound **6h**) resulted in a 2-170-fold reduction in antiproliferative activity against all cancer cell lines, indicating that the methyl and methoxy groups are not bioequivalent at the *para*-position of the phenyl ring. The reduction in activity was more evident, 23- and 170-fold, against A549 and HeLa, respectively, while only a 2-, 3- and 5-fold reduced activity was observed against RS4;11, HT-29 and Jurkat cells.

Compound **6i**, with a methoxy group at the *meta*-position of the phenyl ring, was one to four orders of magnitude less active than the *para*-methoxy isomer **6h**, indicating that the position of the methoxy group was important for *in vitro* activity.

Among the strong electron-withdrawing groups, the small polar nitro substituent, intermediate in size between chlorine and bromine, when placed in the *para*-position of the phenyl ring, furnished a

compound (**6j**) with reduced antiproliferative activity (IC_{50}: 1.1-6.3 μM) relative to the unsubstituted phenyl derivative **6a**.

Inhibition of tubulin polymerization and colchicine binding. To investigate whether the antiproliferative effects of these compounds were related to an interaction with tubulin, compounds **6a-b** and **6d-h** were evaluated for inhibition of the polymerization of tubulin (Table 2). For comparison, CA-4 was examined in contemporaneous experiments as a reference compound. The same derivatives were also examined for inhibitory effects on the binding of [^{3}H]colchicine to tubulin.

Table 2. Inhibition of tubulin polymerization and colchicine binding by compounds **6a-b, 6d-h** and CA-4 (**1a**)

Compound	Tubulin assembly[a] IC_{50}±SD (μM)	Colchicine binding [b] % inhibition±SD
6a	10±2	n.d.
6b	18±1	n.d
6d	3.3±0.3	36±3
6e	2.5±0.3	35±4
6f	2.5±0.2	35±2
6g	0.71±0.05	76±0.7
6h	2.8±0.2	31±3
CA-4	1.2±0.1	98±0.7

[a] Inhibition of tubulin polymerization. Tubulin was at 10 μM.
[b] Inhibition of [^{3}H]colchicine binding. Tubulin, colchicine and tested compound were at 1, 5 and 5 μM, respectively.
n.d.: not determined

Compounds **6e**-**h** strongly inhibited tubulin assembly, with derivative **6g** as the most active of the series, being almost 2-fold more active than CA-4 in this assay (IC_{50}: 0.71 and 1.2 μM for **6g** and CA-4, respectively). Compounds **6e**, **6f** and **6h** were half as active (IC_{50}: 2.5, 2.5 and 2.8 μM, respectively) and **6d** about one-third as active (IC_{50}: 3.3 μM) as CA-4. Compounds **6a** and **6b** showed weak antitubulin polymerization activities (IC_{50}: 10 and 18 μM, respectively), which were consistent with their low antiproliferative activity. Thus, the order of inhibitory effects on tubulin

polymerization was **6g>CA-4>6e=6f=6h>6d>>6a>6b**. This order of activity as inhibitors of tubulin assembly correlates well with their order of activity as antiproliferative agents.

Inhibitory effects on colchicine binding studies were performed on compounds with tubulin assembly IC_{50} <5 μM. Derivative **6g**, the agent with the greatest antiproliferative activity, proved to be the most active inhibitor of the binding of [^{3}H]colchicine to tubulin, since 46 and 76% inhibition occurred with this agent at 1 and 5 μM, respectively. This compound was less potent than CA-4, which in these experiments inhibited colchicine binding by 86 and 98%, respectively, at 1 and 5 μM.

For the tested compounds **6a-b** and **6d-h**, there was a positive correlation between inhibition of both tubulin assembly and colchicine binding and antiproliferative activity. These data are consistent with the conclusion that tubulin was an intracellular target of the tested compounds.

EGFR and VEGFR-2 kinase inhibitory activity assay. Compounds **6a-b** and **6d-h** were further evaluated for their EGFR and VEGFR-2 kinase inhibitory activities. The approved VEGFR-2 and EGFR inhibitory agents sunitinib and erlotinib (**2b**), respectively, were used as positive controls. The data compiled in Table 3 showed potent inhibition of $EGFR^{wt}$ kinase by compounds **6a-b** and **6f-h**, but no inhibition of VEGFR-2 (IC_{50}>1 μM) was observed. All tested molecules, with the exception of **6d** and **6e**, were more potent than sunitinib as EGFR kinase inhibitors, with the 2-thienyl derivative **6b** as the most potent compound of the series. All evaluated molecules showed lower potency than erlotinib, with **6b** about 1.7-fold less potent. Three of these compounds (**6f-h**) were discovered to possess dual EGFR and tubulin polymerization inhibitory activity, and a good correlation was observed between antiproliferative activities, inhibition of tubulin polymerization and inhibition of EGFR binding.

Compound **6g**, with the most potent effect on tubulin polymerization, also exhibited excellent EGFR inhibitory activity, with IC_{50} values of 0.71 μM and 30 nM, respectively. In contrast, compound **6b**, the most active compound as an EGFR inhibitor (IC_{50}: 2.5 nM), was less potent as an inhibitor of tubulin polymerization (IC_{50}: 18 μM). As shown in Table 3, compounds **6d** and **6e**, showed moderate

EGFR inhibitory activities (IC_{50}: 273 and 326 nM, respectively) and similar potent antitubulin potency (IC_{50}: 3.3 and 2.5 μM), while for compound **6h** a good correlation was observed between both its EGFR and antitubulin activities. The SAR analysis derived from the antiproliferative activities of compounds **6d** and **6e** was more consistent with their tubulin inhibition activities, probably due to their potent inhibitory activities against tubulin polymerization but moderate activities against EGFR.

Table 3. EGFR inhibitory activities by compounds **6a-b, 6e-h,** sunitinib and erlotinib (**2b**)

Compound	Inhibition of $EGFR^{wt}$ kinase[a] IC_{50}±SD (nM)
6a	23±4
6b	2.5±0.3
6d	273±35
6e	326±46
6f	10±3
6g	30±5
6h	52±6
Sunitinib (2e)	140±19
Erlotinib (2b)	1.5±2

[a]Values are expressed as the mean ± SD from the dose-response curves of at least two independent experiments.

Compound 6g induced inhibition of EGFR activation in HeLa cells. In order to test the inhibition on the phosphorylation of EGFR and the downstream signaling pathway, we evaluated by western blot analysis the inhibition of EGFR phosphorylation by **6g** in HeLa cells. The cells were treated with different concentration of **6g** (10-1000 nM) and then stimulated with epidermal growth factor (EGF) (50 ng/mL) for 15 min. The results (Figure 4) showed that **6g** strongly inhibited the phosphorylation of EGFR in a concentration dependent manner starting at 50 nM. Erlotinib (1 μM) was taken as reference compound, and erlotinib showed similar inhibitory activity as compound **6g**. These results

demonstrated that **6g**, in addition to its antimitotic activity (see below), is also a potent EGFR inhibitor.

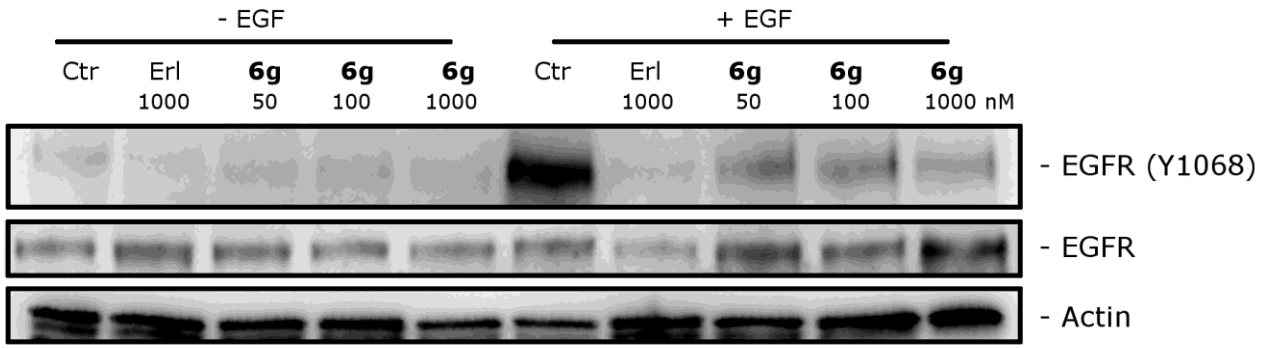

Figure 4. Effects of **6g** on EGFR signaling in HeLa cells. Cells were treated with the indicated concentrations of **6g** for 6 h and then stimulated by EGF (30 ng/mL) for 15 min. Cells were harvested for Western blot analysis for both EGFR and its phosphorylation at Y1068. Erlotinib (Erl) was used as the reference compound. To confirm equal protein loading, each membrane was stripped and reprobed with anti-β-actin antibody.

Molecular modeling. A series of docking simulations were conducted on the newly designed 4-(3',4',5'-trimethoxyanilino)-6-substituted thieno[3,2-*d*]pyrimidines to evaluate their potential interaction with the colchicine site of tubulin.[34] The results showed that the compounds are placed in the active site in a similar manner as the co-crystallized *N*-deacetyl-*N*-(2-mercaptoacetyl)-colchicine (DAMA-colchicine), and the binding mode is consistent with the one previously reported for a thieno[2,3-*b*]pyridine series,[35] with the trimethoxyphenyl group in proximity of βCys241. The thieno[3,2-*d*]pyrimidine core overlapped with the central part of DAMA-colchicine, with the substituted phenyl ring placed in a small hydrophobic sub-pocket, potentially interacting with the surrounding amino acids βThr314, βVal181 and especially βMet259. This small sub-pocket can accommodate the different substituted phenyl rings, but only the *para* methyl derivative **6g** has the correct combination of size/electronic properties to stably occupying and properly fit that area of the binding site (Figure 5C), suggesting a better inhibition of tubulin assembly. Replacement with a larger

methoxy group (**6h**) does not allow the efficient occupation of the sub-pocket, indicating a potential reduction of the inhibition of tubulin polymerization. A similar decrease in activity is seen when the methyl group is replaced by different electron withdrawing atoms (**6d-f**), but in this case the decrease in activity could be associated with the electronic properties of the substituent rather than its size, since they can occupy the sub-pocket very similarly to **6g** (Figure 5B). Compounds where the *para* substituent has been removed (**6a**) or the phenyl ring has been replaced with a smaller 5-member thiophene ring, do not entirely fill the sub-pocket, potentially causing the 10-18 fold activity reduction found for these derivatives (Figure 5A).

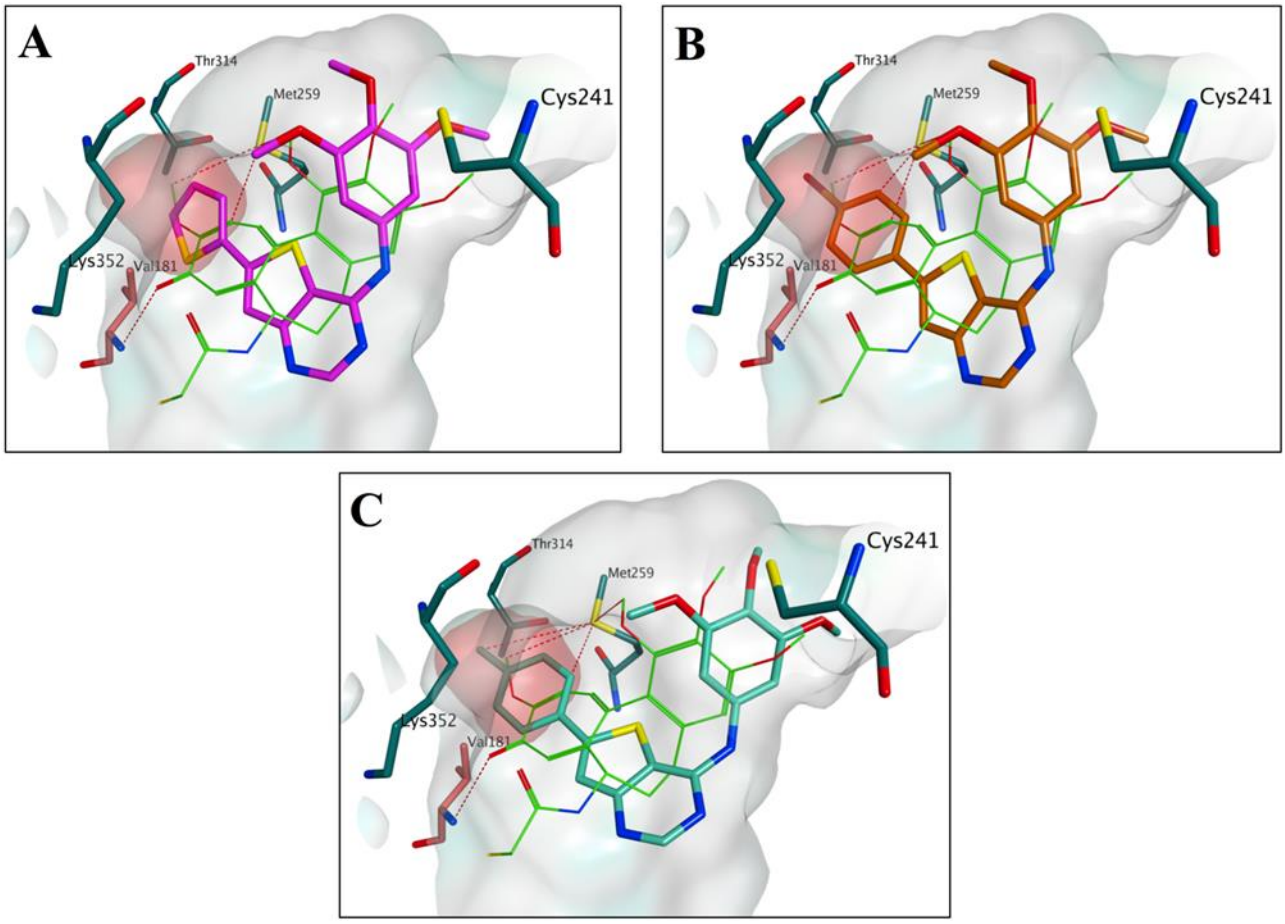

Figure 5. Proposed binding modes for compounds **6b** (**A**), **6e** (**B**) and **6g** (**C**) in comparison with DAMA-colchicine in the colchicine site (PDB ID: 1SA0). Carbons of the co-crystallized DAMA-colchicine are shown in green, of compound **6b** in purple, of compound **6e** in orange and of compound **6g** in turquoise. The residues from the α-tubulin chain are shown in salmon, whereas residues from β-tubulin are colored in teal. The sub-pocket is highlighted with a red surface.

In an attempt to clarify the potential binding mode of the new derivatives in the EGFR kinase domain, docking of the new molecules was performed using the crystal structure of the EGFR kinase domain in complex with the inhibitor (*R*)-6-(4-((4-ethylpiperazin-1-yl)methyl)phenyl)-*N*-(1-phenylethyl)-7*H*-pyrrolo[2,3-*d*]pyrimidin-4-amine (AEE788).[36] The 6-phenyl-thieno[3,2-*d*]pyrimidine core of the molecules perfectly overlaps with the phenyl pyrrolo[2,3-*d*]pyrimidine core of the co-crystallized inhibitor, making the same interactions with Gln791, Met793 and Leu844 that seem to anchor the molecule to the binding site (Figure 6). The trimethoxyphenyl group is placed in the same area occupied by the methyl moiety of AEE788, in proximity of Asp855.

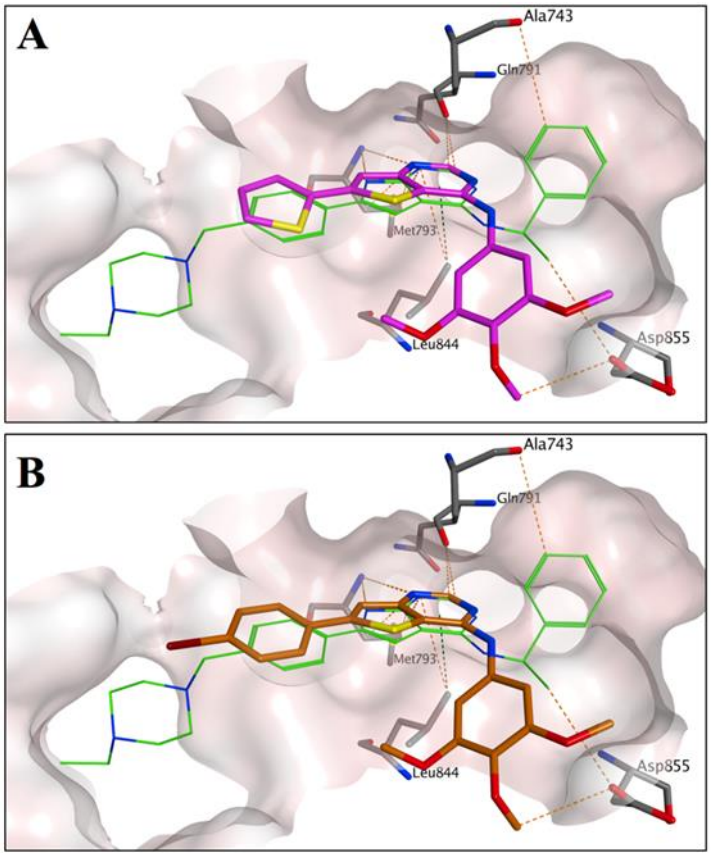

Figure 6. Proposed binding modes for compounds **6b** (**A**) and **6e** (**B**) in comparison with the inhibitor AEE788 in the crystal structure of the EGFR kinase domain (PDB ID: 2J6M). The carbons of the co-crystallized AEE788 are shown in green, of compound **6b** in purple and of compound **6e** in orange. The phenyl ring of **6e** and the thiophene of **6b** are not involved in any interaction with the surrounding residues.

Overall, the binding mode proposed for these compounds is very similar to that of the co-crystallized ligand and also to another previously published thienopyrimidine EGFR inhibitor.[23] All the new compounds occupy the active site in an identical manner. However, from these results, it is not possible to fully rationalize the role of the substitution on the phenyl ring in the anti-EGFR activity, since that part of the molecule does not seem to be involved in any specific interactions with the binding pocket.

Effects of compound 6g on the cell cycle. The effect of the most active compound (**6g**) on cell cycle progression was examined by flow cytometry in Hela and Jurkat cells (Figure 7). After a 24 h treatment, the compound induced a G2/M arrest in both cell lines cells even at 25 nM. A concomitant reduction of cells in both the S and G1 phases was also observed. In order to determine whether **6g** was able to block cells at the mitotic phase (M), cells were stained with an immunofluorescent antibody to p-histone H3, a well-known mitotic marker,[37] as well as propidium iodide (PI), and analyzed by flow cytometry. As shown in Figure 7 (Panel C), in which representative histograms are presented, HeLa cells arrested in M phase by treatment with **6g** are readily distinguished from G2 cells by the higher level of p-histone H3. In particular, treatment with **6g** induced an increase in the percentage of mitotic cells from the about 1.5% observed in untreated cells to about 38% and 50 % with 50 and 100 nM concentrations, respectively, at 24 h (Figure 7, Panel C).

Compound 6g induced apoptosis in different cell lines. To evaluate the mode of cell death induced by the test compounds, we performed a bi-parametric cytofluorimetric analysis using PI and annexin-V-FITC, which stain DNA and phosphatidylserine (PS) residues, respectively. We used two cell lines, Hela and Jurkat, in which we evaluated the effects of compound **6g** after both 24 and 48 h treatments. As shown in Figure 8, in both cell lines, the compound induced apoptosis in a time and concentration dependent manner. The apoptotic effect of **6g** was evident at the lowest concentration examined (50 nM), in good agreement with the cytotoxic potency shown in the (3-(4,5-dimethylthiazol-2-yl)-2,5-diphenyl tetrazolium bromide (MTT) test (Table 1).

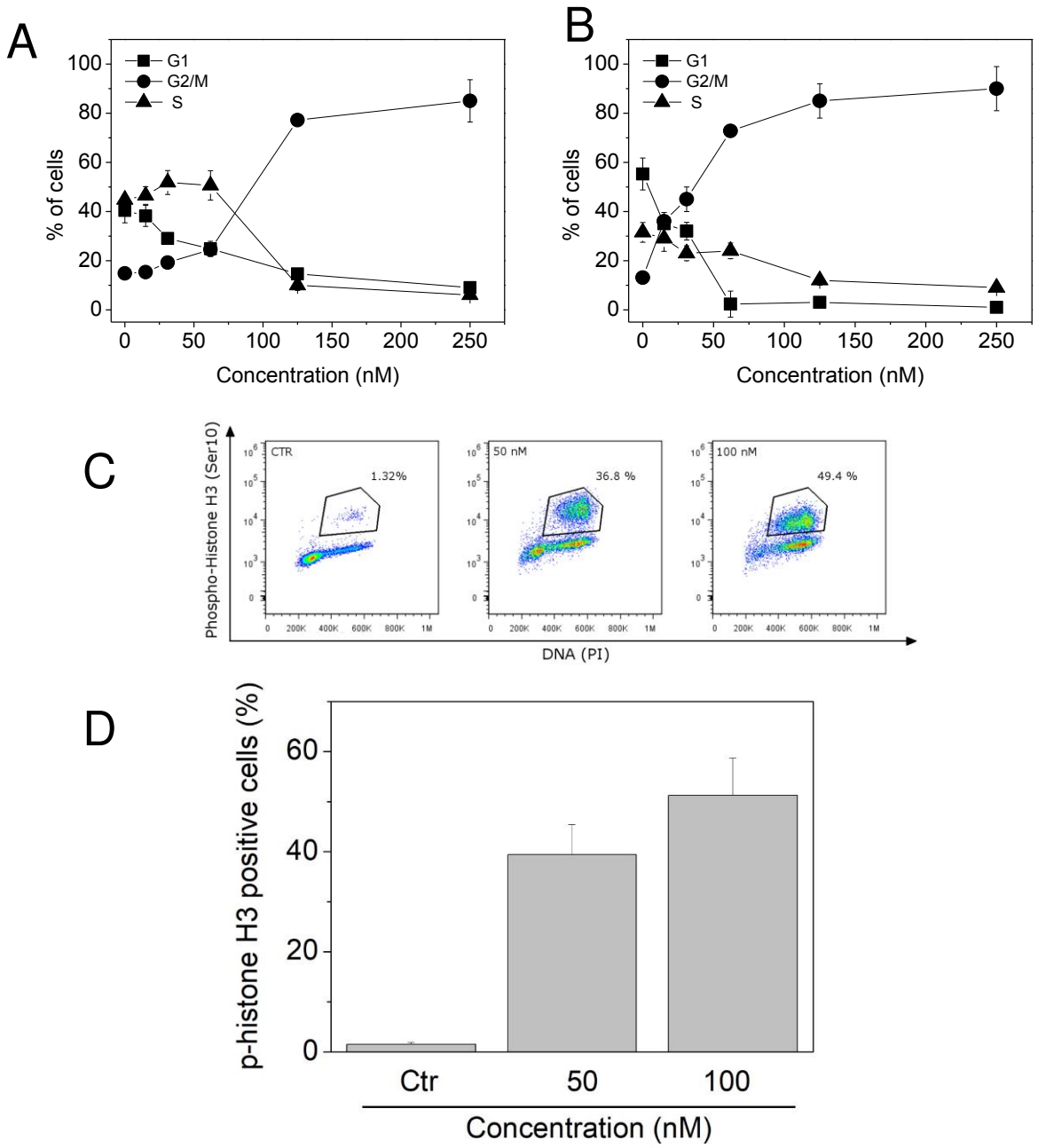

Figure 7. Percentage of cells in each phase of the cell cycle in HeLa (Panel A) and Jurkat cells (Panel B) treated with compound **6g** at the indicated concentrations for 24 h. Cells were fixed and labeled with PI and analyzed by flow cytometry as described in the Experimental Section. Data are presented as mean±SEM of three independent experiments. Representative flow cytometric patterns of mitotic cells with phosphorylated histone-H3 (Panel C) and histograms showing quantitative comparisons (Panel D) after treatment with **6g** at the indicated concentrations in HeLa cells. Data are presented as mean±SEM of two independent experiments.

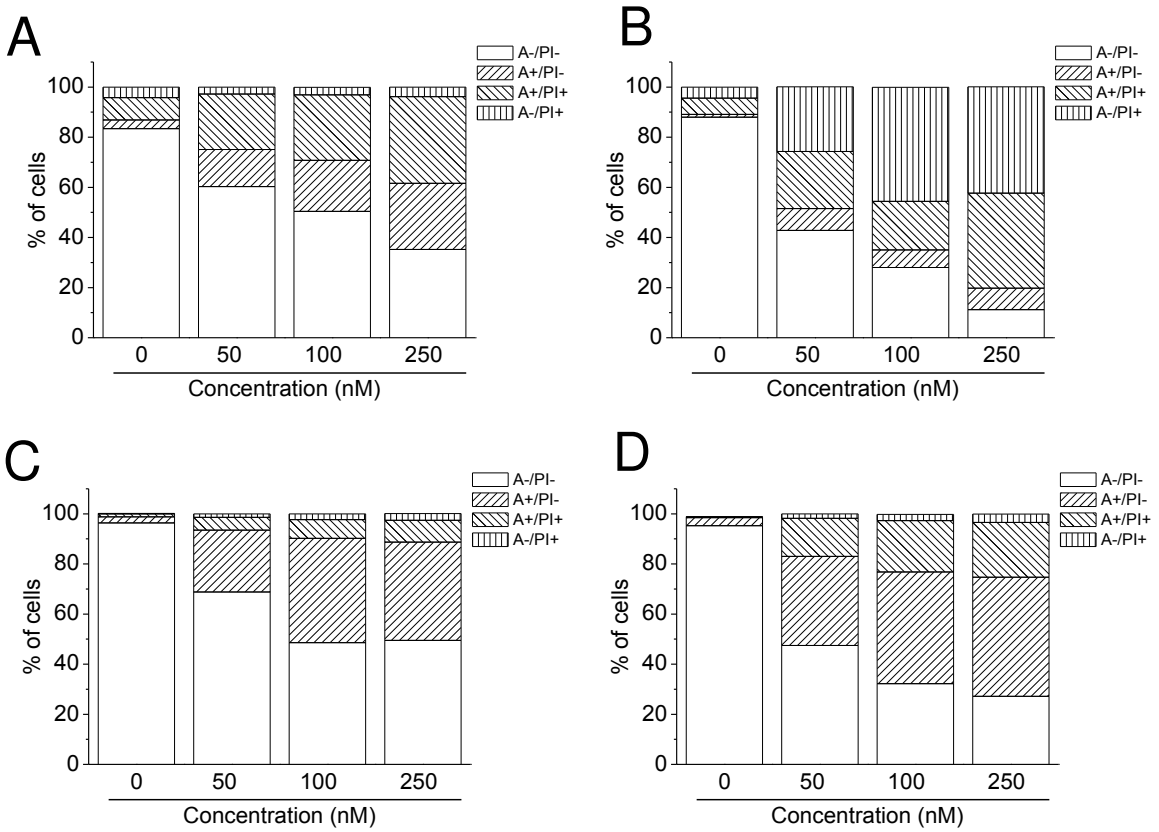

Figure 8. Flow cytometric analysis of apoptotic cells after treatment of HeLa (Panels A and B) and Jurkat (Panels C and D) cells with **6g** at the indicated concentrations after incubation for 24 (Panels A and C) or 48 h (Panels B and D). The cells were harvested and labeled with annexin-V-FITC and PI and analyzed by flow cytometry.

Compound 6g induced mitochondrial depolarization and the production of reactive oxygen species (ROS). Mitochondria play an essential role in the propagation of apoptosis.[38,39] In fact, it is well established that, at an early stage, apoptotic stimuli alter the mitochondrial transmembrane potential ($\Delta\psi_{mt}$). We therefore evaluated by flow cytometry, using the fluorescent dye 5,5',6,6'-tetrachloro-1,1',3,3'-tetraethylbenzimidazolcarbocyanine (JC-1), the variation in $\Delta\psi_{mt}$ upon treatment of HeLa cells with compound **6g**. As shown in Figure 9 (Panel A), cells treated with different concentration of **6g** (50, 100 and 250 nM) showed a concentration- and a time-dependent increase in the percentage of cells with low $\Delta\psi_{mt}$. The depolarization of the mitochondrial membrane is already evident at early times of drug exposure (3-6 h), in good agreement with the concept that the dissipation of $\Delta\psi_{mt}$ is an early event characteristic of apoptosis observed with many microtubule

stabilizing and destabilizing agents in different cell types.[40-42] Since the mitochondrial membrane depolarization is associated with the mitochondrial production of ROS,[43] we investigated whether ROS production increased after treatment with **6g**. As shown in Figure 9 (Panel B) compound **6g** induced significant production of ROS starting at 12-24 h of treatment at 50-250 nM, in good agreement with the mitochondrial depolarization described above.

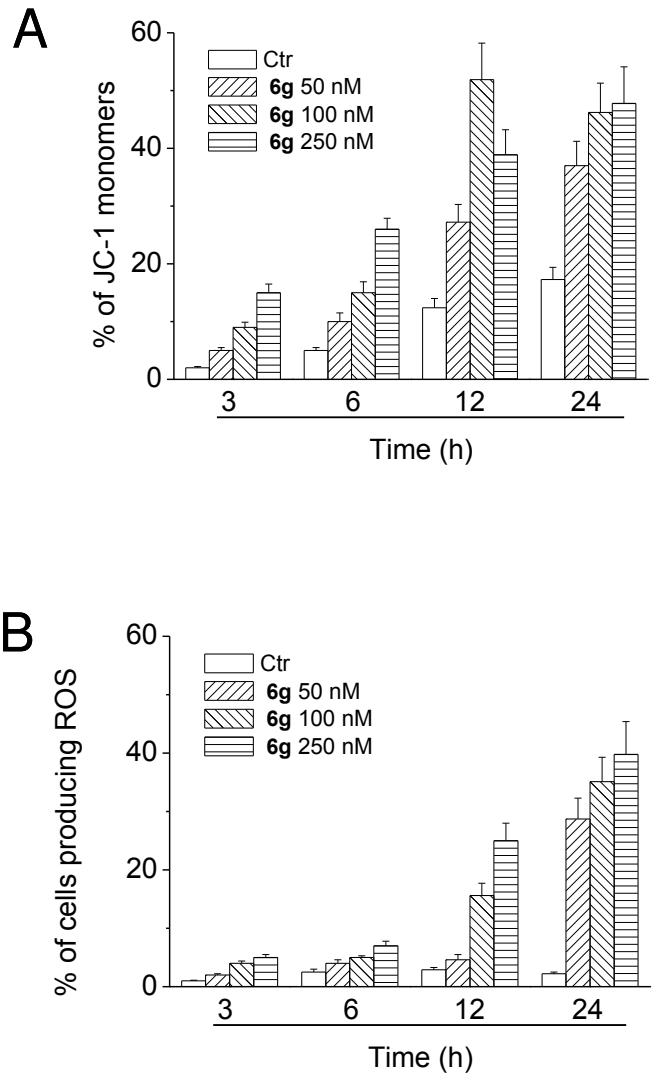

Figure 9. Assessment of mitochondrial membrane potential ($\Delta\psi_{mt}$) (Panel A) and production of ROS (Panel B) after treatment of HeLa cells with compound **6g**. Cells were treated with the indicated concentration of compound for 3, 6, 12 and 24 h and then stained with the fluorescent probe JC-1 for analysis of mitochondrial potential or with 2,7-dichlorodihydrofluorescein diacetate (H_2-DCFDA)

for the evaluation of ROS levels. Cells were then analyzed by flow cytometry as described in the experimental section.

Compound 6g induced PARP activation and caused a decrease in the expression of anti-apoptotic proteins. To gain a better insight into the mechanism of action of **6g**, we evaluated the cleavage of poly(ADP-ribose) polymerase (PARP) during the apoptotic process induced by this compound. As shown in Figure 10, compound **6g** in HeLa cells caused a concentration and time-dependent cleavage of PARP, confirming its pro-apoptotic activity. Moreover, the expression of two anti-apoptotic proteins, Bcl-2 and Mcl-1, was also studied.[44,45] Immunoblot analysis, shown in Figure 10, demonstrated that the expression of the anti-apoptotic protein Bcl-2 was decreased starting after a 24 h treatment at both 50 and 100 nM. The decrease in expression of Mcl-1 was even greater, both at the lowest concentration and after the 24 h treatment.

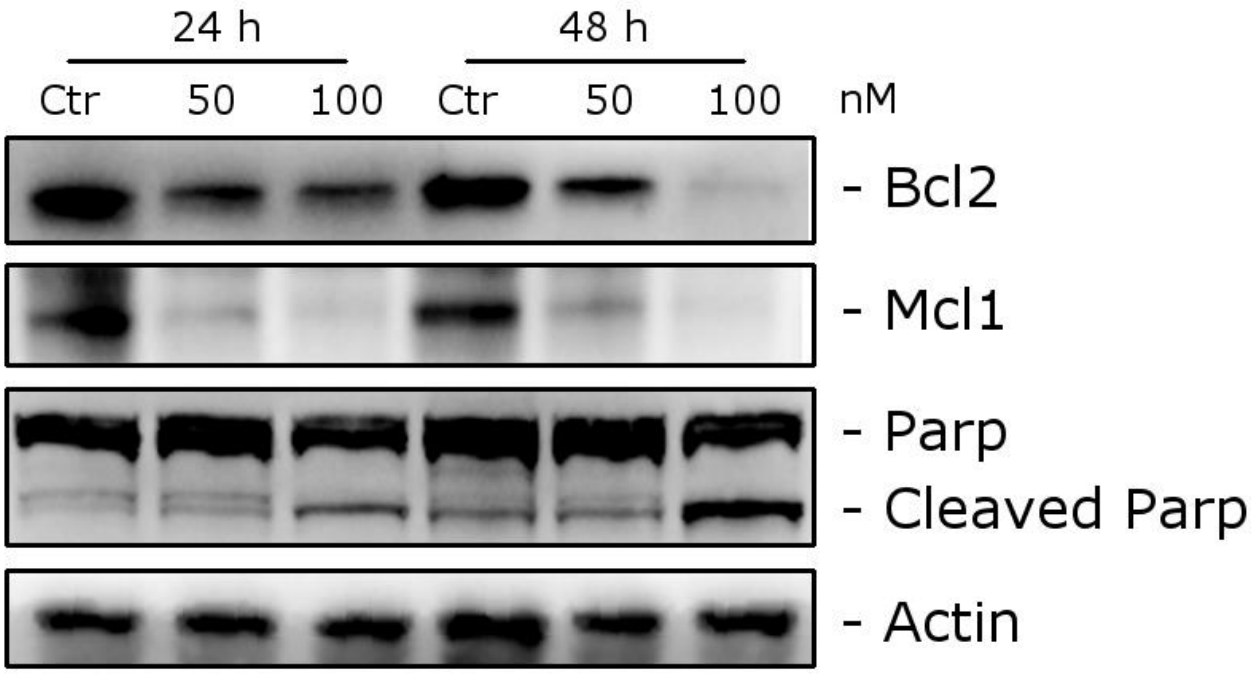

Figure 10. Western blot analysis of PARP, Bcl-2 and Mcl-1 after treatment of HeLa cells with **6g** at the indicated concentrations and for the indicated times. To confirm equal protein loading, each membrane was stripped and reprobed with anti-β-actin antibody.

Derivative 6g had antivascular effects *in vitro*. Recent antitumor strategies have included the use of chemotherapeutics with antiangiogenic or antivascular drugs to increase the efficacy of the treatment,[4] and, in this context, many tubulin binding agents show antivascular effects against tumor endothelium,[46-49] including CA-4. For that reason, we evaluated **6g** for its effects on endothelial cells utilizing HUVECs as a model to study angiogenesis in vitro.

To evaluate the antivascular activity of **6g**, we analyzed the ability of the compound to disrupt the "tubule-like" structures formed by HUVECs seeded on Matrigel. Matrigel is an extracellular matrix rich in pro-angiogenic factors that stimulate single endothelial cells to assume an extended shape and produce a reticulum similar to a capillary network. Preliminary experiments carried out on these cells, with the aim to evaluate the cytotoxicity of the test compound, indicated that **6g** has a GI_{50} of 56 nM, after a 48 h treatment. Thus to evaluate antivascular activity, we used a concentration of **6g** that did not induce cellular death.

As shown in Figure 11 (Panel A), just after a 1 h incubation, compound **6g** at the the noncytotoxic concentration of 10 nM, as well as the cytotoxic concentration of 100 nM, clearly disrupted the network of HUVECs, as compared with the control. Image analysis[49] was performed to obtain a quantitative measurement of the total length of the tubules, the area and the number of meshes, the percent of area covered by HUVECs, and the number of branching points after a 1 h treatment (Figure 11, Panels B-G). The results showed for segment length and meshes area a statistically significant effect for the lowest concentration used, suggesting, the high potential vascular disrupting activity of **6g**.

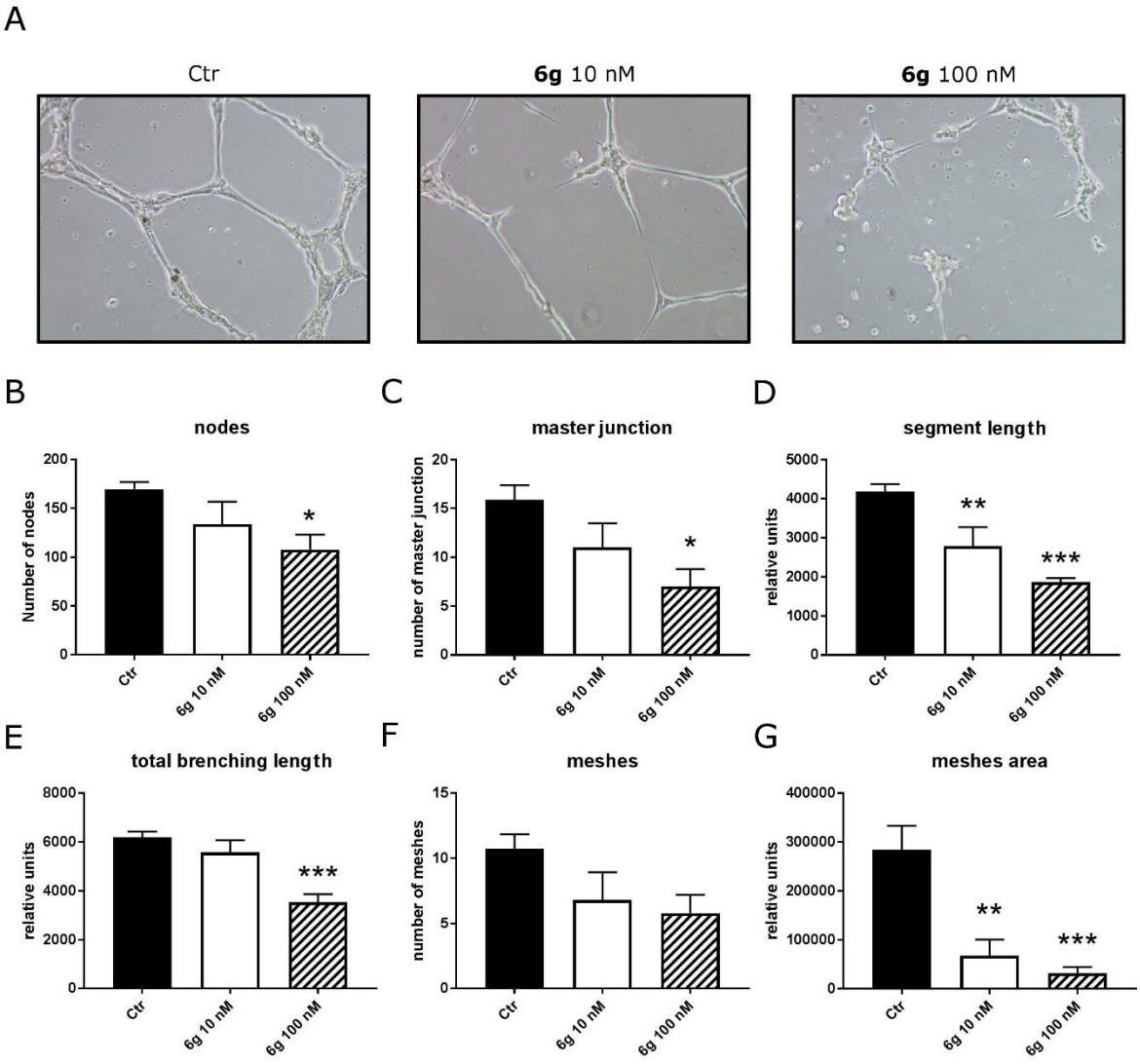

Figure 11. Inhibition of endothelial cell capillary-like tubules formation by **6g**. Tubules formation on Matrigel was carried out as described in Materials and Methods. Panel A. Representative pictures of preformed capillary-like tubules treated with **6g** for 1 h at the concentrations of 10 nM and 100 nM, (add comma) respectively. Panels B-G. quantitative analysis of the effects of **6g** on the dimensional and topological parameters of the preformed capillary-like tubules network. Data are represented as mean ± S.E.M. of three independent experiments. **p<0.01; ***p<0.001

6g induced tumor growth reduction in a mouse allograft tumor model. To evaluate its antitumor effect *in vivo*, **6g** was administered by the intraperitoneal route every other day, starting at day 9, at two different doses (3.0 and 7.5 mg/kg) in an allograft tumor model developed in mice.[50,51] As reference compound, CA-4P was used at 30 mg/kg. This model consists of the use of B16 murine melanoma cells that are injected in the flank of individual mice. This melanoma cell line was selected because it expresses high levels of EGFR.[52] Moreover, in preliminary experiments, we also verified the effectiveness of **6g** on this murine tumor line. The compound had an IC_{50} of 23.4 ± 3.8 nM measured by the MTT assay, indicating that its cytotoxic potency was similar to that found in the human tumor cell lines (see Table 1).

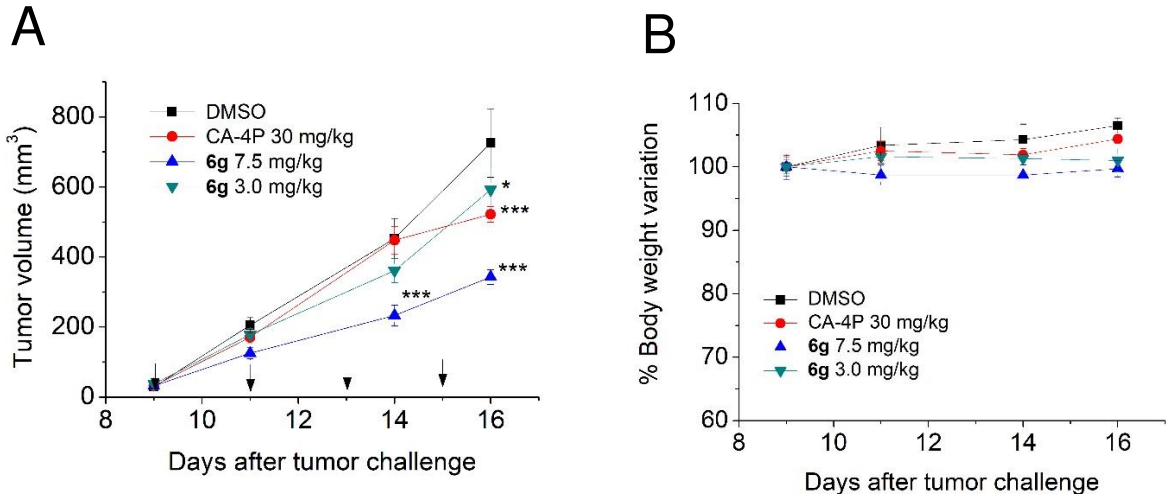

Figure 12. Inhibition of mouse allograft growth *in vivo* by compound **6g**. Male C57BL/6 mice were injected subcutaneously at their dorsal region with $2.5x10^5$ BL6-B16 murine melanoma cells. Tumor-bearing mice were administered the vehicle, as control, or 3 or 7.5 mg/kg of **6g** or 30 mg/kg of CA-4P as reference compound. Injections were given intraperitoneally at the days indicated by the arrows. B) Body weight variation after treatment with compound **6g** as described above. Data are presented as mean ± SEM of tumor volume at each time point for 5 animals per group. *p<0.05, ***p<0.001 *vs*. control.

As shown in Figure 12 (Panel A), after six days of treatment (doses administered on days 9, 11, 13 and 15), **6g** was able to significantly reduce tumor burden in a dose-dependent manner, even at the lowest dose tested (3.0 mg/kg). We observed reduction of tumor mass of 28.0, and 52.5% at the doses

of 3.0 and 7.5 mg/kg, respectively. The reference compound CA-4P at 30 mg/kg induced 34.9% reduction of tumor mass. Notably, the *in vivo* efficacy clearly indicates an increased antitumor efficacy of **6g** as compared with CA-4P. Even at the highest dose, **6g** did not show any sign of toxicity and did not cause a decrease in animal body weight (Figure 12, Panel B).

Conclusions

An effective strategy to develop anticancer agents is the discovery of synergistic multi-targeting properties of new molecules. The thiophene ring has been employed as an isostere for benzene-fused pyrimidines in the design of molecules that possess tyrosine kinase inhibitory activity. In this study we report the design and synthesis of a new series 4-(3',4',5'-trimethoxyanilino)-6-substituted thieno[3,2-*d*]pyrimidines, some of which possess both tubulin polymerization and EGFR kinase inhibitory properties. Structural optimization was conducted with variation in the electron-releasing or electron-withdrawing group on the phenyl at the C-6 position of the 4-(3',4',5'-trimethoxyanilino)-thieno[3,2-*d*]pyrimidine system.

The data shown in Table 1 indicated the importance of substituents on the phenyl at the C-6 position of 4-(3',4',5'-trimethoxyanilino)thieno[3,2-*d*]pyrimidine system for activity and selectivity against different cancer cell lines. Three of the 4-(3',4',5'-trimethoxyanilino)-6-substituted thieno[3,2-*d*]pyrimidine derivatives, corresponding to *p*-Cl (**6d**), *p*-Me (**6g**) and *p*-OMe (**6h**) analogues were more active than the rest of the derivatives, with IC_{50} values of, respectively, 3-600, 1-20 nM and 4-430 nM in the five cell lines. The 4-(3',4',5'-trimethoxyanilino)-6-(*p*-tolyl)thieno[3,2-*d*]pyrimidine derivative **6g** was the most potent compound of the whole series, exhibiting an IC_{50} value of 19 nM against the NSCLC A549 cell line, which harbors $EGFR^{WT}$ and K-ras mutations. Comparing the *p*-tolyl derivative **6g** with the *p*-methoxy phenyl compound **6h**, the latter was 2-170-fold less active than **6g**, with the greatest differences in activity being 23- and 170-fold in A549 and Hela cells, respectively.

The corresponding thieno[2,3-*d*]pyrimidine isomers and the 2-anilino-7-(3',4',5'-trimethoxyanilino)thiazolo[4,5-*d*]pyrimidine derivatives generally had little activity, with IC_{50} values usually greater than 10 μM. There was a considerable difference in potency between 4-(3',4',5'-trimethoxyanilino)-6-arylthieno[3,2-*d*]pyrimidine derivatives **6a**, **6d** (*p*-Cl), **6g** (*p*-Me) and **6h** (*p*-OMe) and the regioisomeric 4-(3',4',5'-trimethoxyanilino)-6-arylthieno[2,3-*d*]pyrimidine analogues **8d**, **8f**, **8i** and **8k**, respectively, with these latter being considerably less active than the former in all cancer cell lines examined.

The inhibitory activity against EGFR and VEGFR-2 kinases of selected compounds **6a-b** and **6d-h** showed that these molecules were selective EGFR inhibitors. Compounds **6f-h** inhibited both EGFR kinase and tubulin polymerization, while derivative **6b** only inhibited EGFR kinase. Compounds **6a-b** and **6d-h** showed lower potency than erlotinib, with derivative **6b** having the greatest inhibitory activity against EGFR kinase, being only slightly less potent than erlotinib (IC_{50}: 2.5 and 1.5 nM, respectively). Besides its potent antiproliferative activity and high competitive inhibitory activity on EGFR, compound **6g** is also an inhibitor of tubulin polymerization through binding to the colchicine site of tubulin, combining EGFR inhibition with antitubulin activity. The IC_{50} of 0.7 μM obtained with **6g** in the tubulin banding assay was almost half that obtained in simultaneous experiments with CA-4 (IC_{50}: 1.2 μM)

In our results with compounds **6f-h** there was a high correlation between the *in vitro* antiproliferative activity against the cancer cell lines and inhibition of tubulin polymerization and EGFR kinase, which suggested that targeting both tubulin and EGFR kinase played major roles in the cancer cell growth inhibitory effects of these three molecules.

Experimental Section

1. Chemistry. *1.1. Materials and Methods.* ^{1}H and ^{13}C NMR data were obtained with a Varian VXR 200 spectrometer and a Varian Mercury Plus 400 spectrometer, respectively. Peak positions are given in parts per million (δ) downfield, and *J* values are given in hertz. Mass spectra were recorded by an

ESI single quadrupole mass spectrometer Waters ZQ 2000 (Waters instruments UK), and the values are expressed as $[M+1]^+$. Melting points (mp) were determined on a Buchi-Tottoli apparatus and are uncorrected. The purity of tested compounds was determined by combustion elemental analyses conducted by the Microanalytical Laboratory of the Department of Chemistry and Pharmaceutical Sciences of the University of Ferrara with a Yanagimoto MT-5 CHN recorder elemental analyzer. All tested compounds yielded data consistent with a purity of at least 95% as compared with the theoretical values. TLC was carried out using glass plates coated with silica gel 60 F_{254} by Merck, and compounds were visualized by UV detection or with aqueous $KMnO_4$. Flash column chromatography was performed using 230-400 mesh silica gel and the indicated solvent system. Organic solutions were dried over anhydrous Na_2SO_4. Solvents and reagents that are commercially available were purchased from Aldrich (Sigma-Aldrich) or Alfa Aesar (Johnson Matthey Company) and were used without further purification unless otherwise noted. Compounds **12a** and **12b** are commercially available. General procedures and references related to the preparation of methyl 3-aminothiophene-5-aryl/heteroaryl-2-carboxylate **9a-j**, ethyl 5-amino-2-anilinothiazole-4-carboxylate **9k-n** and ethyl 2-aminothiophene-3-carboxylate derivatives **12c-l** are reported in the Supporting Information section. Active compounds were not recognized as PAINS according to the Free ADME-Tox Filtering Tool (FAF-Drugs4) program (http://fafdrugs4.mti.univ-paris-diderot.fr/).

1.2. General procedure A for the preparation of compounds 10a-n and 13a-l. A mixture of the appropriate methyl 3-aminothiophene-5-aryl/heteroaryl-2-carboxylate **9a-j**, ethyl 5-amino-2-anilinothiazole-4-carboxylate **9k-n** or ethyl 2-aminothiophene-3-carboxylate derivatives **12a-l** (10 mmol) and formamide (15 mL) was heated at 180 °C for 18 h. After cooling to room temperature, cooled water (15 mL) was added to the reaction mixture. The solid was removed by filtration, washed with water and dried under vacuum for 12 h. The crude residue was suspended in ethyl ether, stirred for 30 min and filtered. The solid was used for the next reaction without further purification.

*6-Phenylthieno[3,2-d]pyrimidin-4(3H)-one (**10a**).* Following general procedure A, compound **10a** was obtained as a yellow solid. Yield: 71%, mp 294 °C. ^{1}H-NMR (d_6-DMSO) δ: 7.48 (m, 3H), 7.35 (m, 3H), 8.17 (s, 1H), 12.6 (bs, 1H). MS (ESI): $[M+1]^+$=229.3.

*6-(Thiophen-2-yl)thieno[3,2-d]pyrimidin-4(3H)-one (**10b**).* Following general procedure A, compound **10b** was obtained as a black solid. Yield: 95%, mp 170 °C. ^{1}H-NMR (d_6-DMSO) δ: 7.63 (dd, J=2.6 and 1,6 Hz, 1H), 7.74 (dd, J=2.6 and 1,6 Hz, 1H), 8.01 (s, 1H), 8.10 (m, 1H), 8.15 (s, 1H), 12.2 (bs, 1H). MS (ESI): $[M+1]^+$=235.3.

*6-(4-Fluorophenyl)thieno[3,2-d]pyrimidin-4(3H)-one (**10c**).* Following general procedure A, compound **10c** was obtained as a brown solid. Yield: 81%, mp >300 °C. ^{1}H-NMR (d_6-DMSO) δ: 7.34 (d, J=8.8 Hz, 2H), 7.83 (s, 1H), 7.93 (m, 2H), 8.17 (s, 1H), 12.6 (bs, 1H). MS (ESI): $[M+1]^+$=247.3.

*6-(4-Chlorophenyl)thieno[3,2-d]pyrimidin-4(3H)-one (**10d**).* Following general procedure A, compound **10d** was obtained as a brown solid. Yield: 89%, mp >300 °C. ^{1}H-NMR (d_6-DMSO) δ: 7.54 (d, J=8.8 Hz, 2H), 7.87 (m, 3H), 8.17 (s, 1H), 11.6 (bs, 1H). MS (ESI): $[M+1]^+$=263.7.

*6-(4-Bromophenyl)thieno[3,2-d]pyrimidin-4(3H)-one (**10e**).* Following general procedure A, compound **10e** was obtained as a yellow solid. Yield: 78%, mp >300 °C.^{1}H-NMR (d_6-DMSO) δ: 7.67 (d, J=8.6 Hz, 2H), 7.80 (d, J=8.6 Hz, 2H), 7.90 (s, 1H), 8.17 (s, 1H), 12.6 (bs, 1H). MS (ESI): $[M+1]^+$=308.2.

*6-(4-Iodophenyl)thieno[3,2-d]pyrimidin-4(3H)-one (**10f**).* Following general procedure A, compound **10f** was obtained as a yellow solid. Yield: 95%, mp >300 °C. ^{1}H-NMR (d_6-DMSO) δ: 7.63 (d, J=8.8 Hz, 2H), 7.87 (m, 3H), 8.17 (s, 1H), 11.4 (bs, 1H). MS (ESI): $[M+1]^+$=279.7.

*6-(4-Tolyl)thieno[3,2-d]pyrimidin-4(3H)-one (**10g**).* Following general procedure A, compound **10g** was obtained as a brown solid. Yield: 83%, mp >300 °C. ^{1}H-NMR (d_6-DMSO) δ: 2.36 (s, 3H), 7.29 (d, J=7.8 Hz, 2H), 7.73 (m, 3H), 8.15 (s, 1H), 12.5 (bs, 1H). MS (ESI): $[M+1]^+$=243.3.

*6-(4-Methoxyphenyl)thieno[3,2-d]pyrimidin-4(3H)-one (**10h**).* Following general procedure A, compound **10h** was obtained as a brown solid. Yield: >95%, mp >300 °C. ^{1}H-NMR (d_6-DMSO) δ: 3.82 (s, 3H), 7.03 (d, J=8.8 Hz, 2H), 7.71 (s, 1H), 7.78 (d, J=8.8 Hz, 2H), 8.14 (s, 1H), 11.8 (bs, 1H). MS (ESI): $[M+1]^+$=259.3.

*6-(3-Methoxyphenyl)thieno[3,2-d]pyrimidin-4(3H)-one (**10i**).* Following general procedure A, compound **10i** was obtained as a brown solid. Yield: >95%, mp 212 °C. ^{1}H-NMR (d_6-DMSO) δ: 3.84 (s, 3H), 7.04 (m, 1H), 7.39 (m, 2H), 7.88 (s, 1H), 7.94 (d, J=8.6 Hz, 1H), 8.17 (s, 1H), 12.0 (bs, 1H). MS (ESI): $[M+1]^+$=259.3.

*6-(4-Nitrophenyl)thieno[3,2-d]pyrimidin-4(3H)-one (**10j**).* Following general procedure A, compound **10j** was obtained as a brown solid. Yield: >95% yield, mp >300 °C. ^{1}H-NMR (d_6-DMSO) δ: 7.18 (d, J=8.8 Hz, 2H), 7.43 (d, J=8.8 Hz, 2H), 7.94 (s, 1H), 10.5 (bs, 1H), 11.4 (bs, 1H). MS (ESI): $[M+1]^+$=274.3.

1.3. General procedure B for the preparation of compounds 11a-n and 14a-l. A mixture of the appropriate thieno[3,2-*d*]pyrimidin-4(3*H*)-one **10a-j**, thiazolo[4,5-*d*]pyrimidin-7(6*H*)-one **10k-n** or thieno[2,3-*d*]pyrimidin-4(3*H*)-one **13a-l** (5 mmol) and $POCl_3$ (30 mL) with 2-3 drops of DMF was refluxed for 6 h. The mixture was cooled, $POCl_3$ was removed under vacuum, the residue obtained was poured into a saturated solution of $NaHCO_3$ and the suspension neutralized with solid $NaHCO_3$. The mixture was extracted with dichloromethane, the organic phase washed with water, brine, dried over Na_2SO_4 and concentrated *in vacuo*. The crude product was stirred for 15 min with ethyl ether (15 mL), and the desired product was obtained after removal of the ether by filtration.

*4-Chloro-6-phenylthieno[3,2-d]pyrimidine (**11a**).* Following general procedure B, compound **11a** was obtained as a brown solid. Yield: 71%, mp 152 °C. ^{1}H-NMR (d_6-DMSO) δ: 7.57 (m, 3H), 6.01 (m, 2H), 8.25 (s, 1H), 9.03 (s, 1H). MS (ESI): $[M+1]^+$=247.7.

*4-Chloro-6-(thiophen-2-yl)thieno[3,2-d]pyrimidine (**11b**).* Following general procedure B, compound **11b** was obtained as an orange solid. Yield: 60%, mp 176 °C. ^{1}H-NMR (d_6-DMSO) δ: 7.79 (m, 2H), 8.11 (s, 1H), 8.36 (dd, J=2.6 and 1,6 Hz, 1H), 9.00 (s, 1H). MS (ESI): $[M+1]^+$=252.7.

*4-Chloro-6-(4-fluorophenyl)thieno[3,2-d]pyrimidine (**11c**).* Following general procedure B, compound **11c** was obtained as a brown solid. Yield: 83%, mp >300 °C. ^{1}H-NMR ($CDCl_3$) δ: 7.37 (d, J=8.8 Hz, 2H), 8.04 (m, 2H), 8.11 (s, 1H), 9.03 (s, 1H). MS (ESI): $[M+1]^+$=265.7.

*4-Chloro-6-(4-chlorophenyl)thieno[3,2-d]pyrimidine (**11d**).* Following general procedure B, compound **11d** was obtained as a yellow solid. Yield: 68%, mp 188 °C.^{1}H-NMR ($CDCl_3$) δ: 7.47 (d, J=8.8 Hz, 2H), 7.69 (m, 3H), 8.96 (s, 1H). MS (ESI): $[M+1]^+$=282.2.

*6-(4-Bromophenyl)-4-chlorothieno[3,2-d]pyrimidine (**11e**).* Following general procedure B, compound **11e** was obtained as a yellow solid. Yield: 55%, mp 201 °C. ^{1}H-NMR (d_6-DMSO) δ: 7.75 (d, J=9.0 Hz, 2H), 7.93 (d, J=9.0 Hz, 2H), 8,29 (s, 1H), 9.04 (s, 1H). MS (ESI): $[M+1]^+$=326.6.

*4-Chloro-6-(4-iodophenyl)thieno[3,2-d]pyrimidine (**11f**).* Following general procedure B, compound **11f** was obtained as a yellow solid. Yield: 54%, mp >300 °C. ^{1}H-NMR ($CDCl_3$) δ: 7.81 (d, J=8.4 Hz, 2H), 7.95 (d, J=8.4 Hz, 2H), 8.29 (s, 1H), 9.04 (s, 1H). MS (ESI): $[M+1]^+$=373.6.

*4-Chloro-6-(p-tolyl)thieno[3,2-d]pyrimidine (**11g**).* Following general procedure B, compound **11g** was obtained as a brown solid. Yield: 84%, mp >300 °C. ^{1}H-NMR (d_6-DMSO) δ: 2.39 (s, 3H), 7.36 (d, J=7.8 Hz, 2H), 7.87 (d, J=7.8 Hz, 2H), 8.18 (s, 1H), 9.01 (s, 1H). MS (ESI): $[M+1]^+$=261.7.

*4-Chloro-6-(4-methoxyphenyl)thieno[3,2-d]pyrimidine (**11h**).* Following general procedure B, compound **11h** was obtained as a yellow solid. Yield: 72%, mp 181 °C. ^{1}H-NMR ($CDCl_3$) δ: 3.89 (s, 3H), 7.04 (d, J=8.8 Hz, 2H), 7.69 (s, 1H), 7.71 (d, J=8.8 Hz, 2H), 8.93 (s, 1H). MS (ESI): $[M+1]^+$=277.7.

*4-Chloro-6-(3-methoxyphenyl)thieno[3,2-d]pyrimidine (**11i**).* Following general procedure B, compound **11i** was obtained as a brown solid. Yield: 61%, mp 153 °C. ^{1}H-NMR ($CDCl_3$) δ: 3.87 (s, 3H), 7.14 (m, 1H), 7.76 (m, 3H), 8.29 (s, 1H), 9.04 (s, 1H). MS (ESI): $[M+1]^+$=277.7.

*4-Chloro-6-(4-nitrophenyl)thieno[3,2-d]pyrimidine (**11j**).* Following general procedure B, compound **11j** was obtained as an orange solid. Yield: >95%, mp >300 °C. ^{1}H-NMR (d_6-DMSO) δ: 8.32 (d, J=8.8 Hz, 2H), 8.36 (d, J=8.8 Hz, 2H), 8.51 (s, 1H), 9.10 (s, 1H). MS (ESI): $[M+1]^+$=292.7.

1.4. General procedure C for the synthesis of compounds 6a-j, 7a-d and 8a-l. A mixture of the appropriate 4-chlorothieno[3,2-*d*]pyrimidine **11a-j**, 7-chlorothiazolo[4,5-*d*]pyrimidine **11k-n** or 4-chlorothieno[2,3-*d*]pyrimidine **14a-l** (1 mmol) and 3,4,5-trimethoxyaniline (2 mmol, 366 mg, 2 equiv.) in *iso*-propanol (5 mL) with a drop of concentrated HCl was refluxed for 18 h and then evaporated to dryness *in vacuo*. The residue was dissolved with dichloromethane, and the organic solution was washed with water, followed by brine, and dried over Na_2SO_4, and the solvent was evaporated. The crude residue was purified by column chromatography on silica gel to furnish the desired compound.

*6-Phenyl-N-(3,4,5-trimethoxyphenyl)thieno[3,2-d]pyrimidin-4-amine (**6a**).* Following general procedure C, the crude residue was purified by flash chromatography, using ethyl acetate as eluent, to furnish **6a** as a yellow solid. Yield: 80%, mp 176 °C. ^{1}H-NMR (d_6-DMSO) δ: 3.67 (s, 3H), 3.79 (s, 6H), 7.22 (s, 2H), 7.51 (m, 3H), 7.85 (m, 2H), 7.90 (s, 1H), 8.59 (s, 1H), 9.64 (s, 1H). ^{13}C-NMR (d_6-DMSO) δ: 55.84 (2C), 60.16, 100.17 (2C), 114.74, 120.50, 126,26 (2C), 129.42 (2C), 129.73,

132.62, 133.91, 135.03, 149.41, 152,57 (2C), 154.46, 154.81, 161.03. MS (ESI): $[M+1]^+$=394.5. Anal. ($C_{21}H_{19}N_3O_3S$) C, H, N.

*6-(Thiophen-2-yl)-N-(3,4,5-trimethoxyphenyl)thieno[3,2-d]pyrimidin-4-amine (**6b**).* Following general procedure C, the crude residue was purified by flash chromatography, using ethyl acetate:petroleum ether 9:1 (v:v) as eluent, to furnish **6b** as a yellow solid. Yield: 69%, mp 211 °C. ^{1}H-NMR ($CDCl_3$) δ: 3.67 (s, 3H), 3.79 (s, 6H), 7.21 (s, 2H), 7.62 (dd, J=5.0 and 1.2 Hz, 1H), 7.76 (m, 1H), 7.78 (s, 1H), 8.06 (dd, J=5.0 and 1.2 Hz, 1H), 8.57 (s, 1H), 9.59 (s, 1H). ^{13}C-NMR ($CDCl_3$) δ: 55.73 (2C), 60.06, 99.97 (2C), 113.98, 120.09, 123.76, 126.04, 128.28, 133.74, 134.07, 135.00, 144.26, 152.47 (2C), 154.36, 154.67, 160.94. MS (ESI): $[M+1]^+$=400.5. Anal. ($C_{19}H_{17}N_3O_3S_2$) C, H, N.

*6-(4-Fluorophenyl)-N-(3,4,5-trimethoxyphenyl)thieno[3,2-d]pyrimidin-4-amine (**6c**).* Following general procedure C, the crude residue was purified by flash chromatography, using ethyl acetate as eluent, to furnish **6c** as a brown solid. Yield: 68%, mp 192 °C. ^{1}H-NMR (d_6-DMSO) δ: 3.65 (s, 3H), 3.77 (s, 6H), 7.19 (s, 2H), 7.37 (t, J=9.2 Hz, 2H), 7.86 (s, 1H), 7.88 (m, 2H), 8.57 (s, 1H), 9.63 (bs, 1H). ^{13}C-NMR (d_6-DMSO) δ: 56.30 (2C), 60.62, 10.67 (2C), 115.18, 116.81, 117.03, 121.13, 128.95, 129.04, 129.75, 134.38, 135.44, 148.68, 153.02, 154.97, 155.26, 161.54, 162.07, 164.53. MS (ESI): $[M+1]^+$=412.4. Anal. ($C_{21}H_{18}FN_3O_3S$) C, H, N.

*6-(4-Chlorophenyl)-N-(3,4,5-trimethoxyphenyl)thieno[3,2-d]pyrimidin-4-amine (**6d**).* Following general procedure C, the crude residue was purified by flash chromatography, using ethyl acetate as eluent, to furnish **6d** as a white solid. Yield: 65%, mp 215 °C. ^{1}H-NMR (d_6-DMSO) δ: 3.67 (s, 3H), 3.79 (s, 6H), 7.20 (s, 2H), 7.58 (d, J=7.2 Hz, 2H), 7.86 (d, J=7.2 Hz, 2H), 7.93 (s, 1H), 8.59 (s, 1H), 9.66 (s, 1H). ^{13}C-NMR (d_6-DMSO) δ: 55.74 (2C), 60.06, 100.14 (2C), 114.80, 121.08 (2C), 127.86 (2C), 129.34 (2C), 131.43, 133.78, 134.18, 134.84, 147.80, 152.47, 154.44, 154.74, 160.87. MS (ESI): $[M+1]^+$=428.9. Anal. ($C_{21}H_{18}ClN_3O_3S$) C, H, N.

*6-(4-Bromophenyl)-N-(3,4,5-trimethoxyphenyl)thieno[3,2-d]pyrimidin-4-amine (**6e**).* Following general procedure C, the crude residue was purified by flash chromatography, using ethyl acetate as eluent, to furnish **6e** as a yellow solid. Yield: 68%, mp 219 °C. ^{1}H-NMR (*d*$_6$-DMSO) δ: 3.67 (s, 3H), 3.79 (s, 6H), 7.20 (s, 2H), 7.71 (d, J=7.8 Hz, 2H), 7.80 (d, J=7,8 Hz, 2H), 7.95 (s, 1H), 8.59 (s, 1H), 9.66 (s, 1H). ^{13}C-NMR (*d*$_6$-DMSO) δ: 55.75 (2C), 60.06, 100.14 (2C), 114.81, 121.08, 122.86, 128.09 (2C), 131.79, 132.25 (2C), 133.87, 134.86, 147.88, 152.47 (2C), 154.46, 154.75, 160.89. MS (ESI): $[M+1]^+$=520.4. Anal. ($C_{21}H_{18}BrN_3O_3S$) C, H, N.

*6-(4-Iodophenyl)-N-(3,4,5-trimethoxyphenyl)thieno[3,2-d]pyrimidin-4-amine (**6f**).* Following general procedure C, the crude residue was purified by flash chromatography, using ethyl acetate:petroleum ether 8:2 (v:v) as eluent, to furnish **6f** as a yellow solid. Yield: 61%, mp 199 °C. ^{1}H-NMR (*d*$_6$-DMSO) δ: 3.67 (s, 3H), 3.79 (s, 6H), 7.20 (s, 2H), 7.84 (d, J=8.4 Hz, 2H), 7.88 (d, J=8.4 Hz, 2H), 7.94 (s, 1H), 8.59 (s, 1H), 9.65 (s, 1H). ^{13}C-NMR (*d*$_6$-DMSO) δ: 55.73 (2C), 60.05, 100.11 (2C), 114.72, 120.91 (2C), 126.14, 127.98 (2C), 129.33, 132.03, 133.84, 134.85, 138.07, 148.14, 152.46, 154.43, 154.72, 160.87. MS (ESI): $[M+1]^+$=520.4. Anal. ($C_{21}H_{18}IN_3O_3S$) C, H, N.

*6-(p-Tolyl)-N-(3,4,5-trimethoxyphenyl)thieno[3,2-d]pyrimidin-4-amine (**6g**).* Following general procedure C, the crude residue was purified by flash chromatography, using ethyl acetate as eluent, to furnish **6g** as a yellow solid. Yield: 75%, mp 202 °C. ^{1}H-NMR (*d*$_6$-DMSO) δ: 2.37 (s, 3H), 3.67 (s, 3H), 3.79 (s, 6H), 7.22 (s, 2H), 7.33 (d, J=8.0 Hz, 2H), 7.74 (d, J=8.0 Hz, 2H), 7.83 (s, 1H), 8.58 (s, 1H), 9.60 (s, 1H). ^{13}C-NMR (*d*$_6$-DMSO) δ: 20.77, 55.73 (2C), 60.05, 99.99 (2C), 114.32, 119.63, 126.04 (2C), 129.78, 129.97 (2C), 133.75, 134.99, 139.47, 149.51, 152.46 (2C), 154.30, 154.64, 161.02. MS (ESI): $[M+1]^+$=408.5. Anal. ($C_{22}H_{21}N_3O_3S$) C, H, N.

*6-(4-Methoxyphenyl)-N-(3,4,5-trimethoxyphenyl)thieno[3,2-d]pyrimidin-4-amine (**6h**).* Following general procedure C, the crude residue was purified by flash chromatography, using ethyl acetate as eluent, to furnish **6h** as a brown solid. Yield: 54%, mp 182 °C. ^{1}H-NMR (*d*$_6$-DMSO) δ: 3.67 (s, 3H),

3.79 (s, 6H), 3.83 (s, 3H), 7.07 (d, J=8.4 Hz, 2H), 7.21 (s, 2H), 7.76 (s, 1H), 7.83 (d, J=8.8 Hz, 2H), 8.56 (s, 1H), 9.56 (s, 1H). ^{13}C-NMR (*d*$_6$-DMSO) δ: 55.31, 55.75 (2C), 60.08, 99.97 (2C), 105.88, 109.63, 114.73 (2C), 118.87 (2C), 125.06, 127.64 (2C), 135.06, 149.46, 152.49, 154.30, 154.58, 160.39, 161.22. MS (ESI): $[M+1]^+$=424.5. Anal. ($C_{22}H_{21}N_3O_4S$) C, H, N.

*6-(3-Methoxyphenyl)-N-(3,4,5-trimethoxyphenyl)thieno[3,2-d]pyrimidin-4-amine (**6i**).* Following general procedure C, the crude residue was purified by flash chromatography, using ethyl acetate as eluent, to furnish **6i** as a yellow solid. Yield: 62%, mp 163 °C. ^{1}H-NMR (*d*$_6$-DMSO) δ: 3.67 (s, 3H), 3.78 (s, 6H), 3.86 (s, 3H), 7.08 (m, 1H), 7.14 (s, 2H), 7.43 (m, 3H), 7.94 (s, 1H), 8.59 (s, 1H), 9.63 (s, 1H). ^{13}C-NMR (*d*$_6$-DMSO) δ: 55.35, 55.85 (2C), 60.16, 100.05 (2C), 111.47, 114.77, 115.56, 118.55, 120.85, 130.61, 133.86, 133.95, 135.08, 149.22, 152.57 (2C), 154.48, 154.78, 159.86, 160.95. MS (ESI): $[M+1]^+$=424.5. Anal. ($C_{22}H_{21}N_3O_4S$) C, H, N.

*6-(4-Nitrophenyl)-N-(3,4,5-trimethoxyphenyl)thieno[3,2-d]pyrimidin-4-amine (**6j**).* Following general procedure C, the crude residue was purified by flash chromatography, using ethyl acetate as eluent, to furnish **6j** as a yellow solid. Yield: 79%, mp >300 °C. ^{1}H-NMR (*d*$_6$-DMSO) δ: 3.67 (s, 3H), 3,80 (s, 6H), 7.21 (s, 3H), 8.12 (d, J=9.0 Hz, 2H), 8.17 (s, 1H), 8.35 (d, J=9.0 Hz, 2H), 8.63 (s, 1H), 9.78 (s, 1H). ^{13}C-NMR ($CDCl_3$) δ: 55.77 (2C), 60.06, 78.53, 78.86, 79.19, 100.32 (2C), 123.48, 124.54 (2C), 127.27 (2C), 134.67, 138.68, 147.53, 152.50 (2C), 154.68, 154.91, 160.63. MS (ESI): $[M+1]^+$=439.4. Anal. ($C_{21}H_{18}N_4O_5S$) C, H, N.

2. Biology. Materials and Methods.

2.1 Antiproliferative assays. Human T-cell leukemia (Jurkat) and human B-cell leukemia (RS4;11) cells were grown in RPMI-1640 medium, (Gibco, Milano, Italy). human non-small cell lung carcinoma (A549), human cervix carcinoma (HeLa) and human colon adenocarcinoma (HT-29) cells were grown in DMEM medium (Gibco, Milano, Italy). Both media were supplemented with 115 units/mL of penicillin G (Gibco, Milano, Italy), 115 μg/mL of streptomycin (Invitrogen, Milano,

Italy) and 10% fetal bovine serum (Invitrogen, Milano, Italy). These cell lines were purchased from ATCC. Stock solutions (10 mM) of the different compounds were obtained by dissolving them in DMSO. Individual wells of a 96-well tissue culture microtiter plate were inoculated with 100 μL of complete medium containing $8x10^3$ cells. The plates were incubated at 37 °C in a humidified 5% CO_2 incubator for 18 h prior to the experiments. After medium removal, 100 μL of fresh medium containing the test compound at different concentrations was added to each well and incubated at 37 °C for 72 h. The percentage of DMSO in the medium never exceeded 0.25%. This was also the maximum DMSO concentration in all cell-based assays described below. Cell viability was assayed by the MTT test as previously described.[35] The IC_{50} was defined as the compound concentration required to inhibit cell proliferation by 50%, in comparison with cells treated with the maximum amount of DMSO (0.25%) and considered as 100% viability.

2.2. Effects on tubulin polymerization and on colchicine binding to tubulin. To evaluate the effect of the compounds on tubulin assembly *in vitro*,[53a] varying concentrations of compounds were preincubated with 10 μM bovine brain tubulin in 0.8 M monosodium glutamate (pH adjusted to 6.6 with HCl in a 2.0 M stock solution) at 30 ˚C and then cooled to 0 ˚C. After addition of 0.4 mM GTP, the mixtures were transferred to 0 °C cuvettes in a recording spectrophotometer and warmed to 30 °C. Tubulin assembly was followed turbidimetrically at 350 nm. The IC_{50} was defined as the compound concentration that inhibited the extent of assembly by 50% after a 20 min incubation. The capacity of the test compounds to inhibit colchicine binding to tubulin was measured as described,[53b] except that the reaction mixtures contained 1 μM tubulin, 5 μM [^{3}H]colchicine and 1 or 5 μM test compound.

2.3. EGFR and VEGFR kinase activity assays. Kinase assays was performed using the bioluminescent ADP-Glo™ kinase assay (Promega, Milano Italy), following the manufacturer's instructions. Assay was performed with the test compounds at different scalar concentrations. The

IC_{50} values reported are based on the average of at least 2 titration curves. As reference compounds erlotinib (Sigma-Aldrich) and sunitinib (Selleckchem, USA) were used.

2.4. Molecular modeling. All molecular docking studies were performed on a Viglen Genie Intel®Core™ i7-3770 vPro CPU@ 3.40 GHz x 8 running Ubuntu 14.04. Molecular Operating Environment (MOE) 2015.10 and Maestro (Schrödinger Release 2017-1) were used as molecular modeling software.[54,55] The tubulin structure and the EGFR kinase domain were downloaded from the PDB data bank (http://www.rcsb.org/; PDB codes 1SA0 and 2J6M, respectively). The two proteins were preprocessed using the Schrödinger Protein Preparation Wizard by assigning bond orders, adding hydrogens and performing a restrained energy minimization of the added hydrogens using the OPLS_2005 force field. Ligand structures were built with MOE and minimized using the MMFF94x force field. The ligands were then prepared using the Maestro LigPrep tool by energy minimizing the structures (OPLS_2005 force filed), generating possible ionization states at pH 7±2, generating tautomers and low-energy ring conformers. A 12 Å docking grid (inner-box 10 Å and outer-box 22 Å) was prepared using as centroid the co-crystallized DAMA-colchicine for the tubulin structure, and a 15 Å docking grid (inner-box 10 Å and outer-box 25 Å) was prepared using as centroid the co-crystallized AEE788 for the EGFR structure. Molecular docking was performed using Glide SP precision keeping the default parameters and setting 5 as the number of output poses per input ligand to include in the solution. The docking results were visually inspected on MOE for their ability to bind the active sites.

2.5. Flow cytometric analysis of cell cycle distribution. 5×10^5 HeLa or Jurkat cells were treated with different concentrations of the test compounds for 24 h. After the incubation period, the cells were collected, centrifuged, and fixed with ice-cold ethanol (70%). The cells were then treated with lysis buffer containing RNase A and 0.1% Triton X-100 and then stained with PI. Samples were analyzed on a Cytomic FC500 flow cytometer (Beckman Coulter). DNA histograms were analyzed using MultiCycle for Windows (Phoenix Flow Systems).

2.6. Apoptosis assay. Cell death was determined by flow cytometry of cells double stained with annexin V/FITC and PI. The Coulter Cytomics FC500 (Beckman Coulter) was used to measure the surface exposure of PS on apoptotic cells according to the manufacturer's instructions (Annexin-V Fluos, Roche Diagnostics).

2.7. Western blot analysis. HeLa cells were incubated in the presence of **6g** and, after different times, were collected, centrifuged, and washed two times with ice cold phosphate buffered saline (PBS). In some experiments Hela cells were treated with **6g** or erlotinib (Sigma-Aldrich) and stimulated with EGF (R&D Systems, Minneapoli MN, USA) 50 ng/mL for 15 min. and then processed as described above. The pellet was then resuspended in lysis buffer. After the cells were lysed on ice for 30 min, lysates were centrifuged at 15000 x g at 4 °C for 10 min. The protein concentration in the supernatant was determined using the BCA Protein Assay (Pierce, Italy). Equal amounts of protein (10 μg) were resolved using sodium dodecyl sulfate-polyacrylamide gel electrophoresis (SDS-PAGE) (Criterion Precast, BioRad, Italy) and transferred to a PVDF Hybond-P membrane (GE Healthcare). Membranes were blocked with a bovine serum albumin solution (5% in Tween PBS 1X), the membranes being gently rotated overnight at 4 °C. Membranes were then incubated with primary antibodies against, PARP, Mcl-1, Bcl-2, (all from Cell Signaling) or β-actin (Sigma-Aldrich) for 2 h at room temperature. Membranes were next incubated with peroxidase labeled secondary antibodies for 60 min. All membranes were visualized using ECL Select (GE Healthcare), and images were acquired using an Uvitec-Alliance imaging system (Uvitec, Cambridge, UK). To ensure equal protein loading, each membrane was stripped and reprobed with an anti-β-actin antibody.

2.8. Evaluation of the antivascular activity *in vitro.* HUVECs were prepared from human umbilical cord veins, as previously described.[46,49] The adherent cells were maintained in M200 medium supplemented with Low Serum Growth Supplement, containing fetal bovine serum, hydrocortisone, hEGF, bFGF, heparin, gentamycin/amphotericin (Life Technologies, Monza, Italy). Once confluent,

the cells were detached by trypsin–EDTA solution and used in experiments from the first to sixth passages.

Matrigel matrix (Basement Membrane Matrix, BD Biosciences, Italy) was kept at 4 °C for 3 h, when 230 µL of Matrigel solution was added to each well of a 24-well plate. After gelling at 37°C for 30 min, gels were overlaid with 500 µL of medium containing 6 x 10^4 HUVECs. The cells were incubated over Matrigel for 6 h to allow capillary tubes to form. Different concentrations of test compound were added in the cultures and incubated for different times, and the disappearance of existing vasculature was monitored and photographed (five fields for each well: the four quadrants and the center) at a 10x magnification. Phase contrast images were recorded using a digital camera and saved as TIFF files. Image analysis was carried out using ImageJ image analysis software, and the following dimensional parameters (percent area covered by HUVECs and total length of HUVECs network per field) and topological parameters (number of meshes and branching points per field) were estimated.[46,49]

2.9. *In vivo* animal studies. Procedures involving animals and their care conformed with institutional guidelines that comply with national and international laws and policies (EEC Council Directive 86/609, OJ L 358, 12 December 1987) and with "ARRIVE" guidelines (Animals in Research Reporting In Vivo Experiments). Six week old C57BL/6 mice (Charles River, Calco) were injected subcutaneously into the dorsolateral flank with 2.5x10^5 BL6-B16 murine melanoma cells in 200 µL of PBS. When tumors were palpable, animals were treated intraperitoneally every other day with different doses of test compounds dissolved in 50 µL of DMSO. Tumors were measured in two dimensions, and tumor volume was calculated according to the formula V=(D x d^2)/2, where D and d are the major and minor perpendicular tumor diameters, respectively.

Supporting information available. The Supporting Information is available free of charge on the ACS Publications website. Antiproliferative activities of compounds **7a-d** (Table 1s) and **8a-l** (Table 2s). General procedures and references related to the preparation of methyl 3-aminothiophene-5-

aryl/heteroaryl-2-carboxylate **9a-j**, ethyl 5-amino-2-anilinothiazole-4-carboxylate **9k-n** and ethyl 2-aminothiophene-3-carboxylate derivatives **12c-l.** Spectral data for the newly synthesized compounds **7a-d**, **10k-n**, **11k-n**, **13a-l** and **14a-l.** ^{1}H-NMR and ^{13}C-NMR spectra of compounds **6a-j.** Elemental microanalyses for compounds **6a-j**, **7a-d** and **8a-l**.

6b-**6e**-**6g**-docking-1SAO (pdb)

6b-**6e**-docking-2J6M (pdb)

Molecular formula strings (CSV).

Author Information

* To whom correspondence should be addressed: (R.R.): Phone: 39-(0)532-455303. Fax: 39-(0)532-455953. E-mail: rmr@unife.it. (L.C.L.C.): Phone: 34-(0)958-243849. Fax: 34-(0)958-243845. E-mail:lcarlotalopez@ugr.es. (G.V.): Phone: 39-(0)49-8215485. Fax: 39-(0)49-8211462. E-mail:giampietro.viola1@unipd.it.

ORCID

Romeo Romagnoli: 0000-0002-6374-773X

Filippo Prencipe: 0000-0001-6426-2761

Paola Oliva: 0000-0002-9148-931X

Stefania Baraldi: 0000-0003-3197-3043

Pier Giovanni Baraldi: 0000-0002-1150-7216

Santiago Schiaffino Ortega: 0000-0002-2583-1084[e]

Mariem Chayah: 0000-0002-1367-8633

Maria Kimatrai Salvador: 0000-0002-3160-4240

Luisa Carlota Lopez-Cara: 0000-0002-6674-4825

Andrea Brancale: 0000-0002-9728-3419

Salvatore Ferla: 0000-0002-5918-9237

Ernest Hamel: 0000-0003-3648-103X

Roberto Ronca: 0000-0001-8979-7068

Roberta Bortolozzi: 0000-0002-3357-4815

Elena Mariotto: 0000-0002-3960-8561

Elena Mattiuzzo: 0000-0002-8205-412X

Giampietro Viola: 0000-0001-9329-165X

Acknowledgment. We wish to thank Alberto Casolari for technical assistance. We also acknowledge the support of the Life Science Research Network Wales grant n^{o}. NRNPGSep14008, an initiative funded through the Welsh Government's Ser Cymru program. We acknowledge "Proyecto de Excelencia de la Consejería de Innovación y Ciencia de la Junta de Andalucía, Spain ref. P12-CTS-696" for its financial support.

Disclaimer. The content of this paper is solely the responsibility of the authors and does not necessarily reflect the official views of the National Institutes of Health.

Abbreviations. CA-4**,** combretastatin A-4; CA-4P, combretastain A-4 disodium phosphate; $\Delta\psi_{mt}$, mitochondrial transmembrane potential; DAMA-colchicine, *N*-deacetyl-*N*-(2-mercaptoacetyl)-colchicine; DMEM, Dulbecco's modified Eagle's medium; DMSO, dimethyl sulfoxide; EGF, epidermal growth factor; $EGFR^{wt}$, epidermal growth factor receptor wild type; ERG, electron-releasing group; ESI, electrospray ionization; EWG, electron-withdrawing group; HER, human epidermal growth factor receptor; H_2DCFDA, 2,7-dichlorodihydrofluorescein diacetate; JC-1, 5,5',6,6'-tetrachloro-1,1',3,3'-tetraethylbenzimidazolcarbocyanine; MTT, (3-(4,5-dimethylthiazol-2-yl)-2,5-diphenyl tetrazolium bromide; NSCLC, nonsmall cell lung cancer; PARP, poly(ADP-ribose) polymerase; PBS, phosphate-buffered saline; PI, propidium iodide; ROS, reactive oxygen species; SAR, structure-activity relationships; VEGFR-2, vascular growth factor receptor-2.

References

1. a) Akhmanova, A.; Steinmetz, M. O. Control of microtubule organization and dynamics: two ends in the limelight. Nat. Rev. *Mol. Cell. Biol.* **2015**, *16*, 711-726; b) Brouhard, G. J.; Rice, L. M. The contribution of αβ-tubulin curvature to microtubule dynamics. *J. Cell Biol.* **2014**, *207*, 323-334.
2. a) Vindya, N. G.; Sharma, N.; Yadav, M.; Ethiraj, K. R. Tubulins-the target for anticancer therapy. *Curr. Top. Med. Chem.* **2015**, *15*, 73-82; b) Nitika, V.; Kapil, K. Microtubule targeting agents: a benchmark in cancer therapy. *Curr. Drug Ther.* **2014**, *8*, 189-196.
3. a) Patil, P. O.; Patil, A. G.; Rane, R. A.; Patil, P. C.; Deshmukh, P. K.; Bari, S. B.; Patil, D. A.; Naphade, S. S. Recent advancement in discovery and development of natural product combretastatin-inspired anticancer agents. *Anticancer Agents Med. Chem.* **2015**, *15*, 955-969; b) Mukhtar, E.; Adhami, V. M.; Mukhtar, H. Targeting microtubules by natural agents for cancer therapy. *Mol. Cancer Ther.* **2014**, 13, 275-284.
4. a) Porcù, E.; Bortolozzi, R.; Basso, G.; Viola, G. Recent advances in vascular disrupting agents in cancer therapy. *Future Med. Chem.* **2014**, *6*, 1485-1498, b) Mita, M. M.; Sargsyan, L.; Mita, A. C.; Spear, M. Vascular disrupting agents in oncology. *Expert. Opin. Invest. Drugs* **2013**, *22*, 317-328.
5. a) Pettit, G. R.; Singh, S. B.; Hamel, E.; Lin, C. M.; Alberts, D. S.; Garcia-Kendall, D. Isolation and structure of the strong cell growth and tubulin inhibitor combretastatin A-4. *Experientia* **1989**, *45*, 209-211; b) Pettit, G. R.; Cragg, G. M.; Herald, D. L.; Schmidt, J. M.; Lohavanijaya, P. Isolation and structure of combretastatin. *Can. J. Chem.* **1982**, *60*, 1374-1376.
6. Lin, C. M.; Ho, H. H.; Pettit, G. R.; Hamel, E. Antimitotic natural products combretastatin A-4 and combretastatin A-2: studies on the mechanism of their inhibition of the binding of colchicine to tubulin. *Biochemistry* **1989**, *28*, 6984-6991.

7. Liu, P.; Qin, Y.; Wu, L.; Yang, S.; Li, N.; Wang, H.; Xu, H.; Sun, K.; Zhang, S.; Han, X.; Sun, Y.; Shi, Y. A phase I clinical trial assessing the safety and tolerability of combretastatin A4 phosphate injections. *Anti-Cancer Drugs* **2014**, *25*, 462-471.

8. a) Patil, P. O.; Patil, A. G.; Rane, R. A.; Patil, P. C.; Deshmukh, P. K.; Bari, S. B.; Patil, D. A.; Naphade, S. S. Recent advancement in discovery and development of natural product combretastatin-inspired anticancer agents. *Anticancer Agents Med. Chem.* **2015**, *15*, 955-969; b) Rajak, H.; Dewangan, P. K.; Patel, V.; Jain, D. K.; Singh, A.; Veerasamy, R.; Sharma, P. C.; Dixit, A. design of combretastatin A-4 analogs as tubulin targeted vascular disrupting agent with special emphasis on their cis-restricted isomers. *Curr. Pharm. Des.* **2013**, *19*, 1923-1955.

9. Greene, L. M.; Meegan, M. J.; Zisterer, D. M. Combretastatins: more than just vascular targeting agents? *J. Pharmacol. Exp. Ther.* **2015**, *355*, 212-227.

10. Field, J. J.; Kanakkanthara, A.; Miller, J. H. Microtubule-targeting agents are clinically successful due to both mitotic and interphase impairment of microtubule function. *Bioorg. Med. Chem.* **2014,** *22*, 5050-5059.

11. a) Goffin, J. R.; Zbuk, K. Epidermal growth factor receptor: pathway, therapies, and pipeline. *Clin. Ther.* **2013**, *35*, 1282-1303; b) Reardon, D. A.; Wen, P. Y.; Mellinghoff, I. K. Targeted molecular therapies against epidermal growth factor receptor: past experiences and challenges. *Neuro Oncol.* **2014**, *16*, viii7-viii13.

12. Hynes, N. E.; Horsch, K.; Olayioye, M. A.; Badache, A. The ErbB receptor tyrosine family as signal integrators. *Endocr. Relat. Cancer* **2001**, *8*, 151-159.

13. a) Hynes, N. E.; Lane, H. A. ERBB receptors and cancer: the complexity of targeted inhibitors. *Nat. Rev. Cancer* **2005**, *5*, 341-354; b) Arteaga, C. L. Epidermal growth factor receptor dependence in human tumors: more than just expression? *Oncologist* **2002**, *4*, 31-39.

14. Olayioye, M. A.; Neve, R. M.; Lane, H. A. N.; Hynes, N. E. The ErbB signaling network: receptor heterodimerization in development and cancer. *EMBO J.* **2000**, *13*, 3159-3167.

15. a) Zhang, H. Three generations of epidermal growth factor receptor tyrosine kinase inhibitors developed to revolutionize the therapy of lung cancer. *Drug Des. Devel. Ther.* **2016**, *10*, 3867-3872; b) Hossam, M.; Lasheen, D. S.; Abouzid, K. A. Covalent EGFR inhibitors: binding mechanisms, synthetic approaches, and clinical profiles. *Arch. Pharm.* **2016**, *349*, 573-593; c) Liu, F.; Tang, B.; Liu, H.; Li, L.; Liu, G.; Cheng, Y.; Xu, Y.; Chen, W.; Huang, Y. 4-Anilinoquinazoline derivatives with epidermal growth factor receptor inhibitor activity. *Anticancer Agents Med. Chem.* **2016**, *16*, 1652-1664.

16. a) Herbst, R. S.; Heymach, J. V.; Lippman, S. M. Lung cancer, N. Engl. J. Med. 2008, 13, 1367-1380; b) Di Maio, M.; Gridelli, C.; Normanno, N.; Perrone, F.; Ciardiello, F. Trying to compose the puzzle with all the pieces: epidermal growth factor tyrosine kinase inhibitors in non-small cell lung cancer. *J. Cell. Physiol.* **2005**, *205*, 355-363: c) Cataldo, V. D.; Gibbons, D. L.; Perez-Soler, R.; Quintas-Cardama, A. Treatment of non-small-cell lung cancer with erlotinib or gefitinib. *N. Engl. J. Med.* **2011**, *364*, 947-955.

17. a) Yun, C. H.; Mengwasser, K. E. Toms, A. V.; Woo, M. S.; Greulich, H.; Wong, K. K.; Meyerson, M., Eck, M. J. The T790M mutation in EGFR kinase causes drug resistance by increasing the affinity for ATP. *Proc. Natl. Acad. Sci. U.S.A.* **2008**, *105*, 2070-2075; Trusolino, L.; Bertotti, A. Compensatory pathways in oncogenic kinase signaling and resistance to targeted therapies: six degrees of separation. *Cancer Discovery* **2012**, *2*, 876-880.

18. The identification numbers in https://clinicaltrials.gov/ are: NCT02326285, NCT00720304, NCT00049283, NCT02319577, NCT00083057, NCT01405079, NCT01755923, NCT00532441, NCT01749072, NCT01050322, NCT00446225 and NCT00553358.

19. a) Litvinov, V. P. The chemistry of thienopyrimidines, Adv. Heterocycl. Chem. 2006, 92, 83-143, b) El-Ansary, A. K.; Kamal, A. M.; Al-Ghorafi, M. A. Synthesis and evaluation of 4-anilinoquinazoline bioisosteres as potential anti-breast cancer agents. *Eur. J. Med. Chem.* **2014**, *86*, 202-210; c) Liu, Z.; Wu, S.; Wang, Y.; Li, R.; Wang, J.; Wang, L.; Zhao, Gong, P.

Design, synthesis and biological evaluation of novel thieno[3,2-*d*]pyrimidine derivatives possessing diaryl semicarbazone scaffolds as potent antitumor agents. *Eur. J. Med. Chem.* **2014**, *87*, 782-799.

20. a) Bugge, S,; Kaspersen, S. J.; Larsen, S.; Nonstad, U.; Bjørkøy, G.; Sundby, E.; Hoff, B. H, Structure-activity study leading to identification of a highly active thienopyrimidine based EGFR inhibitor. *Eur. J. Med. Chem.* **2014**, *75*, 354-374; b) Rheault, T. R.; Caferro, T. R.; Dickerson, S. H.; Donaldson, K. H.; Gaul, M. D.; Goetz, A. S.; Mullin, R. J.; McDonald, O. B.; Petrov, K. G.; Rusnak, D. W.; Shewchuk, L. M.; Spehar, GH. M.; Truesdale, A. T.; Vanderwall, D. E.; Wood, E. R.; Uehling, D. E. Thienopyrimidine-based dual EGFR/ErbB-2 inhibitors. *Bioorg. Med. Chem. Lett.* **2009**, *19*, 817-820; c) Beckers, T.; Sellmer, A.; Eichhorn, E.; Pongratz, H.; Schaechtele, C.; Totzke, F.; Kelter, G.; Krumbach, R.; Fiebig, H. H.; Boehmer, F. D.; Mahboobi, S. Novel inhibitors of epidermal growth factor receptor: (4-(arylamino)-7*H*-pyrrolo[2,3-*d*]pyrimidin-6-yl)(1*H*-indol-2-yl)methanones and (1*H*-indol-2-yl)(4-(phenylamino) thieno[2,3-*d*]pyrimidin-6-yl)methanones. *Bioorg. Med. Chem.* **2012**, *20*, 125-136; d) Milik, S.A., Abdel-Aziz, A.K.; Lasheen, D.S.; Serya, R.A.T.; Minucci, S.; Abouzid, K.A.M. Surmounting the resistance against EGFR inhibitors through the development of thieno[2,3-*d*]pyrimidine-based dual EGFR/HER2 inhibitors. *Eur. J. Med. Chem.* **2018**, *155*, 316-336.

21. Munchhof, M. J.; Beebe, J. S.; Casavant, J. M.; Cooper, B. A.; Doty, J. L.; Higdon, R. C.; Hillerman, S. M.; Soderstrom, C. I.; Knauth, E. A.; Marx, M. A.; Rossi, A. M.; Sobolov, S. B.; Sun, J. Design and SAR of thienopyrimidine and thienopyridine inhibitors of VEGFR-2 kinase activity. *Bioorg. Med. Chem. Lett.* **2004**, *14*, 21-24.

22. Kemnitzer, W.; Sirisoma, N.; May, C.; Tseng, B.; Drewe, J. ; Xiong Cai, S. Discovery of 4-anilino-*N*-methylthieno[3,2-*d*]pyrimidines and 4-anilino-*N*-methylthieno[2,3-*d*]pyrimidines as potent apoptosis inducers. *Bioorg. Med. Chem. Lett.* **2009**, *19*, 3536-3540.

23. Bugge, S.; Formo Buene, A.; Jurisch-Yaksi, N.; Ullestad Moen, I.; Skjønsfjell, E. M.; Sundby, E.; Hoff, B. H. Extended structure-activity study of thienopyrimidine-based EGFR inhibitors with evaluation of drug-like properties. *Eur. J. Med. Chem.* **2016**, *107*, 255-274.

24. Lin, R.; Johnson, S. G.; Connolly, P. J.; Wetter, S. K.; Binnun, E.; Hughes, T. V.; Murray, W. V.; Pandey, N. B.; Moreno-Mazza, S. J.; Adams, M.; Fuentes-Pesquera, A. R.; Middleton, S. A. Synthesis and evaluation of 2,7-diamino-thiazolo[4,5-*d*] pyrimidine analogues as anti-tumor epidermal growth factor receptor (EGFR) tyrosine kinase inhibitors. *Bioorg. Med. Chem. Lett.* **2009**, *19*, 2333-2337.

25. a) Cushman, M.; Nagarathnam, D.; Gopal, D.; He, H.-M.; Lin, C. M.; Hamel, E. Synthesis and evaluation of analogues of (*Z*)-1-(4-methoxyphenyl)-2-(3,4,5-trimethoxyphenyl)ethene as potential cytotoxic and antimitotic agents. *J. Med. Chem.* **1992**, *35*, 2293-2306; b) Hatanaka, T.; Fujita, K.; Ohsumi, K.; Nakagawa, R.; Fukuda, Y.; Nihei, Y.; Suga, Y.; Akiyama, Y.; Tsuji, T. Novel B-ring modified combretastatin analogues: synthesis and antineoplastic activity. *Bioorg. Med. Chem. Lett.* **1998**, *8*, 3371-3374; c) Negi, A. S.; Gautam, Y.; Alam, S.; Chanda, D.; Luqman, S.; Sarkar, J.; Khan, F.; Konwar, R. Natural antitubulin agents: Importance of 3,4,5-trimethoxyphenyl fragment. *Bioorg. Med. Chem.* **2015**, *23*, 373-389.

26. Devambatla, R. K. V.; Choudhary, S.; Ihnat, M.; Hamel, E.; Mooberry, S. L. Gangjee, A. Design, synthesis and preclinical evaluation of 5-methyl-N^4-aryl-furo[2,3-*d*]pyrimidines as single agents with combination chemotherapy potential. *Bioorg. Med. Chem. Lett.* **2018**, *28*, 3085-3093.

27. Pavana, R. K.; Choudhary, S.; Bastian, A.; Ihnat, M. A.; Bai, R.; Hamel, E.; Gangjee, A. Discovery and preclinical evaluation of 7-benzyl-*N*-(substituted)-pyrrolo[3,2-*d*]pyrimidin-4-amines as single agents with microtubule targeting effects along with triple-acting angiokinase inhibition as antitumor agents. *Bioorg Med Chem.* **2017**, *25*, 545-556.

28. Zhang, X.; Raghavan, S.; Ihnat, M.; Hamel, E.; Zammiello, C.; Bastian, A.; Mooberry, S. L.; Gangjee, A. The design, synthesis and biological evaluation of conformationally restricted 4-substituted-2,6-dimethylfuro[2,3-*d*]pyrimidines as multi-targeted receptor tyrosine kinase and microtubule inhibitors as potential antitumor agents. *Bioorg. Med. Chem.* **2015**, *23*, 2408-2423.

29. Ihmaid, S.; Ahmed, H. E. A.; Zayed, M. F. The design and development of potent small molecules as anticancer agents targeting EGFR TK and tubulin polymerization. *Int. J. Mol. Sci.* **2018**, *19*, 408.

30. Mphahlele, M. J.; Maluleka, M. M.; Parbhoo, N.; Malindisa, S. T. Synthesis, evaluation for cytotoxicity and molecular docking studies of benzo[*c*]furan-chalcones for potential to inhibit tubulin polymerization and/or EGFR-tyrosine kinase phosphorylation. *Int. J. Mol. Sci.* **2018**, *19*, 2552.

31. Zayed, M. F.; Ahmed, S.; Ihmaid, S.; Ahmed, H. E. A.; Rateb, H. S.; Ibrahim, S. R. M. Design, synthesis, cytotoxic evaluation and molecular docking of new fluoroquinazolinones as potent anticancer agents with dual EGFR kinase and tubulin polymerization inhibitory effects. *Int. J. Mol. Sci.* **2018,** *19*, 1731.

32. Zayed, M. F.; Rateb, H. S.; Ahmed, S.; Khaled, O. A.; Ibrahim, S. R. M. Quinazolinone-amino acid hybrids as dual inhibitors of EGFR kinase and tubulin polymerization. *Molecules* **2018**, *23*, 1699.

33. Alswah, M.; Bayoumi, A.H.; Elgamal, K.; Elmorsy, A.; Ihmaid, S.; Ahmed, H. E. A. Design, synthesis and cytotoxic evaluation of novel chalcone derivatives bearing triazolo[4,3-*a*]-quinoxaline moieties as potent anticancer agents with dual EGFR kinase and tubulin polymerization inhibitory effects. *Molecules* **2018**, *23*, 48.

34. Ravelli, R.B.; Gigant, B.; Curmi, P.A.; Jourdain, I.; Lachkar, S.; Sobel, A.; Knossow. M. Insight into tubulin regulation from a complex with colchicine and a stathmin-like domain. *Nature* **2004**, *428*, 198-202.

35. Romagnoli, R.; Baraldi, P. G.; Kimatrai Salvador, M.; Preti, D.; Aghazadeh Tabrizi, M.; Bassetto, M.; Brancale, A.; Hamel, E.; Castagliuolo, I.; Bortolozzi, R.; Basso, G.; Viola, G. . Synthesis and biological evaluation of 2-alkoxycarbonyl-3-Anilino benzo[*b*]thiophenes and thieno[2,3-*c*]pyridines as new potent anticancer agents. *J. Med. Chem.* **2013**, *56*, 2606-2618.

36. Yun, C.-H.; Boggon, T. J.; Li, Y.; Woo, S.; Greulich, H.; Meyerson,M.; Eck, M. J. Structures of lung cancer-derived Egfr mutants and inhibitor complexes: mechanism of activation and insights into differential inhibitor sensitivity. *Cancer Cell* **2007**, *11*, 217-227.

37. Goto, H; Tomono, Y.; Ajiro, K.; Kosako H.; Fujita M.; Sakurai, M.; Okawa K.; Iwamatsu, A.; Okigaki, T.; Takahashi, T., Inagaki, M. Identification of a novel phosphorylation site on histone H3 coupled with mitotic chromosome condensation. *J. Biol. Chem.* **1999**, *274*, 25543-25549.

38. Xiong, S., Mu, T.; Wang, G.; Jiang, X. Mitochondria-mediated apoptosis in mammals. *Protein Cell* **2014**, *5*, 737-749.

39. Rovini, A., Savry, A., Braguer, D., Carré, M. Microtubule-targeted agents: when mitochondria become essential to chemotherapy. *Biochim. Biophys. Acta-Bioenerg.* **2011**, *1807*, 679-688.

40. Mendez, G., Policarpi, C., Cenciarelli, C., Tanzarella, C.; Antoccia, A. Role of Bim in apoptosis induced in H460 lung tumor cells by the spindle poison combretastatin-A4. *Apoptosis* **2011**, *16*, 940-949.

41. Romagnoli, R.; Baraldi, P. G.; Kimatrai Salvador, M.; Preti, D.; Tabrizi, M. A.; Brancale, A.; Fu, X.-H.; Li, J.; Zhang, S.-Z.; Hamel, E.; Bortolozzi, R.; Porcù, E.; Basso, G.; Viola, G. Discovery and optimization of a series of 2-aryl-4-amino-5-(3',4',5'-trimethoxybenzoyl)thiazoles as novel anticancer agents *J. Med. Chem.* **2012**, *55*, 5433-5445.

42. Romagnoli, R.; Baraldi, P. G.; Kimatrai Salvador, M.; Prencipe, F.; Bertolasi, V.; Cancellieri, M.; Brancale, A.; Hamel, E.; Castagliuolo. I.; Consolaro, F.; Porcù, E.; Basso, G.; Viola, G. Synthesis, antimitotic and antivascular activity of 1-(3',4',5'-trimethoxybenzoyl)-3-arylamino-5-amino-1,2,4-triazoles. *J. Med. Chem* **2014**, *57*, 6795-6808.

43. Zamzami, N.; Marchetti, P.; Castedo, M.; Decaudin, D.; Macho, A.; Hirsch, T.; Susin, S.A.; Petit, P. X.; Mignotte,B.; Kroemer, G. Sequential reduction of mitochondrial transmembrane potential and generation of reactive oxygen species in early programmed cell death. J. *Exp. Med.* **1995**, *182*, 367-377.

44. Wertz, I. E.; Kusam, S.; Lam, C., Okamoto, T.; Sandoval, W., Anderson, D. J.; Helgason, E., Ernst, J. A.; Eby, M.; Liu, J.; Belmont, L. D.; Kaminker, J. S.; O'Rourke, K. M.; Pujara, K.; Kohli, P. B.; Johnson, A. R.; Chiu, M. L.; Lill, J. R.; Jackson, P. K.; Fairbrother, W. J.; Seshagiri, S.; Ludlam, M. J.; Leong, K. G., Dueber, E. C.; Maecker, H.; Huang, D. C.; Dixit, V. M.. Sensitivity to antitubulin chemotherapeutics is regulated by MCL1 and FBW7. *Nature* **2011**, *471*, 110-114.

45. Czabotar, P. E., Lessene, G., Strasser, A.; Adams, J. M. Control of apoptosis by the BCL-2 protein family: implications for physiology and therapy. *Nature Rev. Mol. Cell Biol.* **2014**, *15*, 49-63.

46. Porcù, E.; Viola, G.; Bortolozzi, R.; Mitola, S.; Ronca, R.; Presta, M.; Persano, L.; Romagnoli, R.; Baraldi, P. G.; Basso, G. TR-644 a novel potent tubulin binding agent induces impairment of endothelial cells function and inhibits angiogenesis. *Angiogenesis* **2013**, *16*, 647-662.

47. Romagnoli, R.; Baraldi, P.G.; Kimatrai Salvador, M.; Prencipe, F.; Bertolasi, V.; Cancellieri, M.; Brancale, A.; Hamel, E.; Castagliuolo, I.; Consolaro, F.; Porcù, E.; Basso, G.; Viola, G. Synthesis, antimitotic and antivascular activity of 1-(3',4',5'-trimethoxybenzoyl)-3-arylamino-5-amino-1,2,4-triazoles. *J. Med. Chem* **2014**, *57*, 6795-6808.

48. Romagnoli, R.; Baraldi, P.G.; Kimatrai Salvador, M.; Schiaffino Ortega, S.; Prencipe, F.; Brancale, A.; Hamel, E.; Castagliuolo, I.; Mitola, S.; Ronca, R.; Bortolozzi, R.; Porcù, E.;

Basso, G.; Viola, G. Design, synthesis, *in vitro* and *in vivo* anticancer and antiangiogenic activity of novel 3-arylamino benzofuran derivatives targeting the colchicine site on tubulin *J. Med, Chem.* **2015**, *58*, 3209-3222.

49. Porcù, E.; Persano, L.; Ronca, R.; Mitola S.; Bortolozzi R., Romagnoli R., Oliva P., Basso G., Viola G. The novel antitubulin agent TR-764 strongly reduces tumor vasculature and inhibitis HIF-1α activation. *Sci. Rep.* **2016**, *6*, 27886.

50. Ronca, R.; Di Salle, E.; Giacomini, A.; Leali, D.; Alessi, P.; Coltrini, D.; Ravelli, C.; Matarazzo, S.; Ribatti, D.; Vermi, W.; Presta, M. Long pentraxin-3 inhibits epithelial-mesenchymal transition in melanoma cells. *Mol. Cancer Ther.* **2013**, *12*, 2760-2771.

51. Romagnoli, R.; Baraldi, P. G.; Prencipe, F.; Lopez-Cara L. C.; Ferla, S.; Brancale, A.; Hamel, E.; Ronca, R.; Bortolozzi, R.; Mariotto. E.; Basso, G.; Viola, G. Design and synthesis of potent in vitro and in vivo anticancer agents based on 1-(3',4',5'-trimethoxyphenyl)-2-aryl-1*H*-imidazole. *Sci. Rep.* **2016**, *6*, 26602.

52. Xu, Q.; Zhang, X.; Yue, J.; Liu C.; Cao C.; Zhong, H.; Qingjun Ma Q. Human TGFalpha-derived peptide TGFalphaL3 fused with superantigen for immunotherapy of EGFR-expressing tumours. *BMC Biotechnology* **2010**, *10*, 91.

53. a) Hamel, E. Evaluation of antimitotic agents by quantitative comparisons of their effects on the polymerization of purified tubulin. *Cell Biochem. Biophys.* **2003**, *38*, 1-21; b) Verdier-Pinard, P.; Lai J.-Y.; Yoo, H.-D.; Yu, J.; Marquez, B.; Nagle D. G.; Nambu, M.; White, J. D.; Falck, J. R.; Gerwick, W. H.; Day, B. W.; Hamel, E. Structure-activity analysis of the interaction of curacin A, the potent colchicine site antimitotic agent, with tubulin and effects of analogs on the growth of MCF-7 breast cancer cells. *Mol. Pharmacol.* **1998**, *53*, 62-67.

54. Molecular Operating Environment (MOE 2015.10); Chemical Computing Group, Inc.: Montreal, Quebec, Canada; URL http://www.chemcomp.com (2015).

55. Schrödinger Release 2017-1: Maestro, Schrödinger, LLC, New York, NY, 20167.

Table of Contents Graphic